

***IN VIVO* MAGNETIC RESONANCE SPECTROSCOPY STUDIES OF THE GLUTAMATE AND GABA NEUROTRANSMITTER CYCLES AND FUNCTIONAL NEUROENERGETICS**

**DOUGLAS L. ROTHMAN
FAHMEED HYDER
NICOLA SIBSON
KEVIN L. BEHAR
GRAEME F. MASON
JUN SHEN
OGNEN A. C. PETROFF
ROBERT G. SHULMAN**

In the last 5 years there has been a renewed interest in the role of metabolism in supporting brain function. Much of this interest is based on the development of functional positron emission tomography (PET) and magnetic resonance imaging (MRI). Although often incorrectly described as directly mapping neuronal activity, both functional PET and MRI actually measure changes in either glucose metabolism or physiologic parameters coupled to glucose metabolism such as blood flow and volume (1). A major limitation in interpreting functional imaging is that the relationship between neuronal activity and the neuroenergetic processes supported by glucose metabolism is poorly defined (2,3). The term *neuronal activity* applies to a spectrum of energy-requiring processes including action potential propagation, neurotransmitter release and uptake, vesicular recycling, and maintenance of membrane potentials (4). All of these processes are involved in short-term neuronal information transfer, and the relative distribution of energy among them remains an open question. There is also uncertainty as to how the different classes of neurons in a region contribute to the overall energy consumption. While an increase in the imaging signal is usually assigned to an increase in neuronal excitation, this interpretation is confounded by both inhibi-

tory and excitatory neuronal function requiring energy. Observation of a regional increase or decrease of the functional imaging signal is not sufficient to distinguish these possibilities. Glia also requires energy, and the relationship between its energy demands and neuronal activity remains to be established. Given these uncertainties about the meaning of the signal at a neuronal level, the validity of functional imaging as a tool for studying mental processes has been largely established based on agreement with prior expectation from psychological paradigms (3,5).

An alternative approach for imaging brain function, which has the potential of directly measuring metabolic pathways involved in excitatory and inhibitory neurotransmission, is *in vivo* magnetic resonance spectroscopy (MRS). MRS uses technology similar to that of the more familiar MRI. It differs by allowing the measurement of the concentrations and synthesis rates of individual chemical compounds within precisely defined regions in the brain. The basis of its chemical specificity is that the resonance frequency of an MRS active nucleus depends not only on the local magnetic field strength, but also on its chemical environment, a phenomenon referred to as chemical shift. MRS measurements of the ^1H nucleus are the most commonly used for *in vivo* studies due to ^1H being the most sensitive nucleus present in biological systems. Metabolites that can be measured by ^1H MRS include aspartate, γ -aminobutyric acid (GABA), glucose, glutamate, glutamine, and lactate. These metabolites play critical roles in neuroenergetics, amino acid neurotransmission, and neuromodulation. Another nucleus of importance for *in vivo* MRS studies is the

Douglas L. Rothman, Fahmeed Hyder, Kevin L. Behar, Graeme F. Mason, Ognen A. C. Petroff, Robert G. Shulman: Yale University School of Medicine, New Haven, Connecticut.

Nicola Sibson: University of Oxford, Oxford, United Kingdom.

Jun Shen: Nathan S. Kline Institute for Psychiatric Research, Orangeburg, New York.

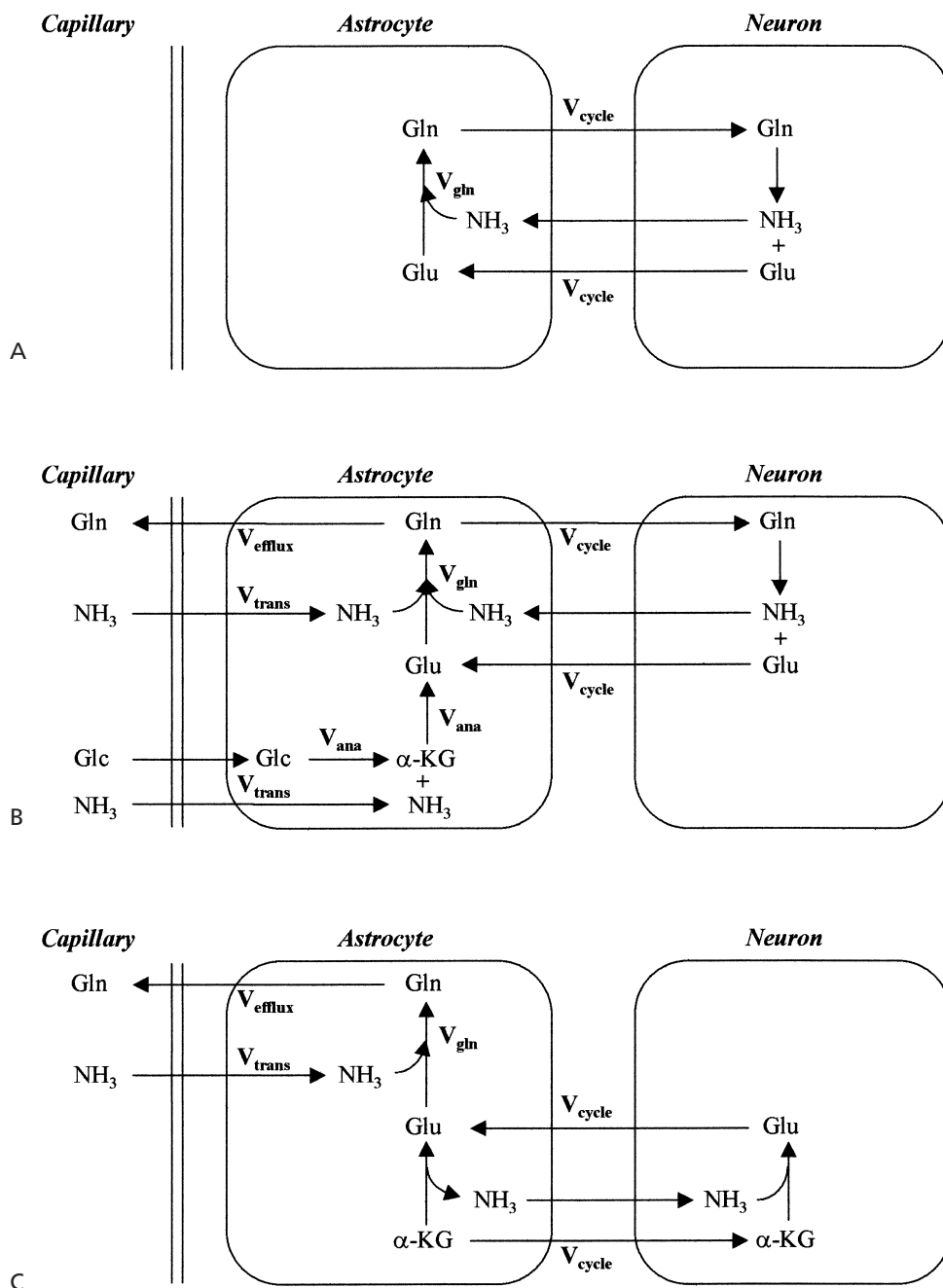


FIGURE 25.1. Schematic representations of the glutamate/glutamine cycle between neurons and astrocytes and the detoxification pathway of glutamine synthesis. **A:** The glutamate/glutamine cycle between neurons and astrocytes. Released neurotransmitter glutamate is transported from the synaptic cleft by surrounding astrocytic end processes. Once in the astrocyte, glutamate is converted to glutamine by glutamine synthetase. Glutamine is released by the astrocyte, transported into the neuron, and converted to glutamate by phosphate-activated glutaminase (PAG), which completes the cycle. **B:** Including the ammonia detoxification (or anaplerotic) pathway of glutamine synthesis. The net rate of glutamine synthesis reflects both neurotransmitter cycling (V_{cycle}) and anaplerosis (V_{ana}). The stoichiometric relationships required by mass balance between the net balance of ammonia and glutamine and V_{ana} are given in Eq. 2. **C:** An alternative model for neuronal glutamate repletion in which the astrocyte repletes the lost neuronal glutamate by providing the neuron with α -ketoglutarate [or equivalently other tricarboxylic acid cycle (TCA) intermediates] (32–34). α -Ketoglutarate is converted back to glutamate by neuronal glutamate dehydrogenase. Glc, glucose; α -KG, α -ketoglutarate; V_{trans} , net rate of net ammonia transport into the brain (VN_{H4} in the text); V_{efflux} , rate of glutamine efflux from the brain; V_{ana} , anaplerotic flux; V_{cycle} , rate of the glutamate/glutamine cycle; V_{gln} , rate of glutamine synthesis. Using [2-¹³C] glucose (27) and [2-¹³C] acetate precursors these pathways may now be distinguished.

^{13}C nucleus. The natural abundance of the ^{13}C isotope is 1.1% so that in conjunction with the infusion of ^{13}C -enriched substrates the rates of isotopic incorporation into brain metabolites can be measured. Substrates labeled with the nonradioactive, stable, ^{13}C isotope have been employed *in vivo* to study metabolic flux, enzyme activity, and metabolic regulation in the living brain of animals and humans (6–39). Enhanced sensitivity may be achieved by measuring the ^{13}C enrichment of a molecule through indirect detection through ^1H MRS. From these measurements the flux through specific metabolic pathways may be calculated (17, 18).

This chapter covers the recent development of *in vivo* MRS to study neuronal glutamate and GABA metabolism and the relationship of amino acid metabolism to functional neuroenergetics. The brain pools of GABA, glutamate, and glutamine have been shown to be localized within glutamatergic neurons, GABAergic neurons, and glia, respectively (under nonpathologic conditions). Under nonfasting conditions glucose is the almost exclusive source of energy for the brain. By following the flow of ^{13}C label from glucose into these metabolites, MRS has been used to determine the separate rates of glucose oxidation in these cell types. The metabolism of glutamatergic neurons, GABAergic neurons, and glia is coupled by neurotransmitter cycles. In the glutamate/glutamine cycle, glutamate released from nerve terminals (by either vesicular release or transport reversal) is transported into surrounding glial cells, and converted to glutamine. Glutamine is then transported out of the glia and into the neurons, where it is converted back to glutamate, thereby completing the cycle (Fig. 25.1). By following the flow of ^{13}C label from glutamate into glutamine, the rate of the glutamate/glutamine cycle may be determined using MRS. Through a similar strategy the GABA/glutamine cycle may be measured.

The application of MRS to study brain glutamate and GABA metabolism and the coupling of neurotransmitter cycling to neuroenergetics have provided several new and controversial insights into the relationship of brain metabolism and function. Contrary to the previous view of a separate metabolic and neurotransmitter pool of glutamate, glutamate release and recycling have been shown to be a major metabolic pathway. MRS studies of GABA metabolism in the rodent and human brain have suggested that there is also an important role of the metabolic pool of GABA in inhibitory function. Another key finding is that the glutamate/glutamine cycle in the cerebral cortex is coupled in a close to 1:1 ratio to neuronal (primarily glutamatergic) glucose oxidation above isoelectricity. This finding, in combination with cellular studies, has led to a model for the coupling between functional neuroenergetics and glutamate neurotransmission. The coupling between neurotransmission and neuroenergetics provides a linkage between the functional imaging signal and specific neuronal processes.

This chapter reviews these findings and discusses some of their implications for functional imaging.

MRS is a low spatial resolution method, with a resolution for studying neurotransmitter systems of approximately 1 to 4 mm³ in animal models and 7 to 40 mm³ in human brain. Even in the best case the MRS signal is the sum of the signal from a large number of neurons and glia including many different subtypes. Fortunately, nature has localized key enzymes and metabolites involved in neurotransmitter cycling in specific cell types, which greatly simplifies the interpretation of the MRS measurements. The evidence of the cellular compartmentalization of metabolism largely derives from invasive methods with cellular and subcellular resolution, which are reviewed here. As with any new technique there are still uncertainties due to methodologic issues. Studies performed to validate the MRS measurements will be reviewed, and present limits in measurement accuracy and interpretation delineated.

IN VIVO ^{13}C MRS MEASUREMENTS OF THE PATHWAYS OF GLUCOSE OXIDATION: FINDINGS AND VALIDATION

This section reviews studies in which MRS was used to measure the pathways of glucose oxidation in the cerebral cortex. Glucose oxidation under nonfasting conditions is almost the exclusive source of energy for the brain. The localization of key enzymes involved in GABA and glutamate metabolism in specific cell types provides the capability for MRS to study their separate neuroenergetic requirements. As shown in Fig. 25.2, which is a ^{13}C MRS spectrum obtained by Gruetter and co-workers (35) at 4 T, the chemical specificity of MRS allows the flow of ^{13}C label from glucose to be followed into several metabolites in the brain coupled to energy metabolism including aspartate, GABA, glutamate, and glutamine. The major finding of these studies is that in normal conditions in nonactivated human cerebral cortex and in rodent models, glucose oxidation in glutamatergic neurons accounts for between 60% and 80% of cerebral cortex energy consumption. The remaining 20% to 40% is primarily distributed between GABAergic neurons and glia.

MRS Measurement of the Rate of Glucose Oxidation in Glutamatergic Neurons

The initial use of MRS to study brain metabolism was to measure glucose oxidation by following the flow of ^{13}C isotope from [1- ^{13}C] glucose into the C4 position of glutamate (2,6). Figure 25.3 diagrams the flow of ^{13}C label from a [1- ^{13}C] glucose precursor to C4-glutamate and subsequently C4-glutamine. Glucose is metabolized to pyruvate by the glycolytic pathway, which labels C3-pyruvate. The

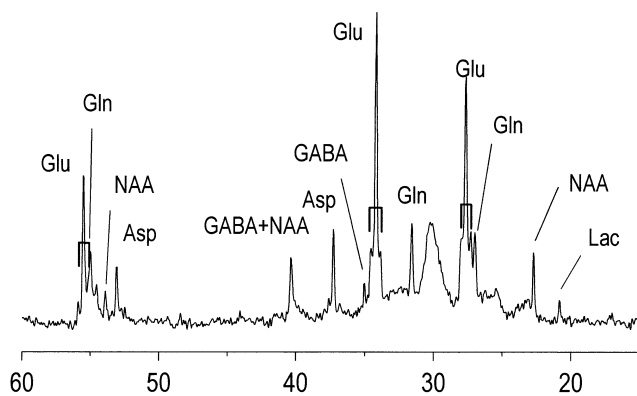


FIGURE 25.2. ^{13}C magnetic resonance spectroscopy (MRS) spectrum in the occipital/parietal lobe at 4 T. The figure shows a 50-minute accumulation ^{13}C MRS spectrum obtained at 4 T approximately 60 minutes after the start of a $1\text{-}^{13}\text{C}$ glucose infusion. The spectrum was obtained from a 72-mL volume centered on the midline in the occipital/parietal lobe. The top trace is an expansion of regions of the bottom trace. Labeled resonances include the C2, C3, and C4 positions of glutamate, glutamine, aspartate, and γ -aminobutyric acid (GABA) and the C3 position of lactate. As described in the text (see *In Vivo ^{13}C MRS Measurements of the Pathways of Glucose Oxidation: Findings and Validation*), the localization of the synthetic enzymes and pools of GABA and glutamine to GABAergic neurons and glia, respectively, and the localization of the majority of the glutamate pool to glutamatergic neurons, allows the relative rates of glucose oxidation in these cell types to be determined from the flow of ^{13}C label into these pools. (From Gruetter R, Seaquist ER, Kim S, et al. Localized in vivo ^{13}C -NMR of glutamate metabolism in the human brain: initial results at 4 tesla. *Dev Neurosci* 1999;20:380–388, with permission.)

label is then transferred to the tricarboxylic acid cycle (TCA) by the actions of pyruvate dehydrogenase (PDH) and citrate synthase. When the label reaches C4- α -ketoglutarate it is transferred to the large neuronal glutamate pool by the high activity exchange reactions of the amino acid transaminases and mitochondrial/cytosolic transporters. The large glutamate pool was first identified in ^{14}C tracer studies (40). Based on kinetic and immunohistochemical staining studies, it is believed to correspond to the glutamate pool of glutamatergic neurons (18,41,42). Due to the rate of these exchange reactions being many times faster than the TCA cycle the glutamate pool acts as a label trap for isotope that enters the neuronal TCA cycle via pyruvate dehydrogenase (17,18). ^{13}C MRS may be used to measure the accumulation of ^{13}C label into the trapping glutamate pool, and the kinetic curves analyzed by metabolic modeling to calculate the rate of the neuronal TCA cycle (18). The trapping pool assumption is not essential to determine the rate of the TCA cycle because subsequent labeling in the C3 position of glutamate can be measured to allow calculation of the label exchange rate (17,18). Because glucose is the primary fuel for neuronal oxidation, the measurements of the TCA cycle may be converted to measurements of glucose oxidation using known stoichiometries (17,18).

The rate of neuronal glucose oxidation has been determined in several studies from ^{13}C MRS and $^1\text{H-}^{13}\text{C}$ MRS measurements of cerebral cortex glutamate turnover from a [$1\text{-}^{13}\text{C}$] glucose precursor in animal models (2,14–17, 21,22,25–27) and humans (12,13,18,19,29,31,35,43,44). Comparison of the rates of neuronal glucose oxidation measured in these studies with conventional arteriovenous (AV) difference and PET measurements of total glucose consumption found that the majority (between 70% and 90%) of total glucose oxidation in the rat and human brain is associated with the large glutamate pool, believed to reflect glutamatergic neurons, measured by MRS. In two recent ^{13}C MRS studies of resting awake human occipital parietal cortex, in which other pathways of glucose metabolism were directly measured, a similar range of between 60% (35) and 80% (29) of total glucose oxidation was calculated for the large glutamate pool. The large percentage of cortical synapses that are glutamatergic and the high electrical activity of glutamatergic pyramidal cells (4,45) may explain why such a large fraction of total glucose oxidation is associated with glutamatergic neurons.

A caveat to the interpretation of the glutamate turnover measurement is that glutamate is present in all brain cells. Based on the sensitivity limitations of staining methods and kinetic studies in measuring glutamate levels in glia and other neuron types, particularly GABAergic, the assignment of the fraction of glucose oxidation occurring in glutamatergic neurons may be overestimated by up to 20%. In the future, the fraction of glutamate in glia may be measured more accurately through dynamic ^{13}C MRS measurements of glutamate and glutamine labeling during the infusion of labeled acetate that is incorporated into the brain selectively in the glia (28,38,39).

MRS Measurements of the Rate Glucose Oxidation in GABAergic Neurons

GABA is the major inhibitory neurotransmitter and may represent over 30% of the synapses in the cerebral cortex (4, 46,47). GABA is synthesized from glutamate in GABAergic neurons by the enzyme glutamic acid decarboxylase (GAD). GABA may then be returned to the TCA cycle through successive action of the GABA shunt enzymes, GABA-transaminase, and succinic semialdehyde dehydrogenase, or released from the neuron. Almost all of the brain GABA pool is localized to GABAergic neurons under normal conditions. The labeling of the GABA pool from [$1\text{-}^{13}\text{C}$] glucose provides a minimum estimate of the rate of glucose oxidation in the GABAergic neuron. The estimate is a minimum because label may bypass GABA and continue from α -ketoglutarate/glutamate into the TCA cycle directly. *In vitro* MRS analysis of cerebral cortex from extracts of rats infused with [$1\text{-}^{13}\text{C}$] glucose has been used to measure the time course of labeling in the GABA and glutamate pools (24, 48). The isotopic labeling results of the Manor et al. (24)

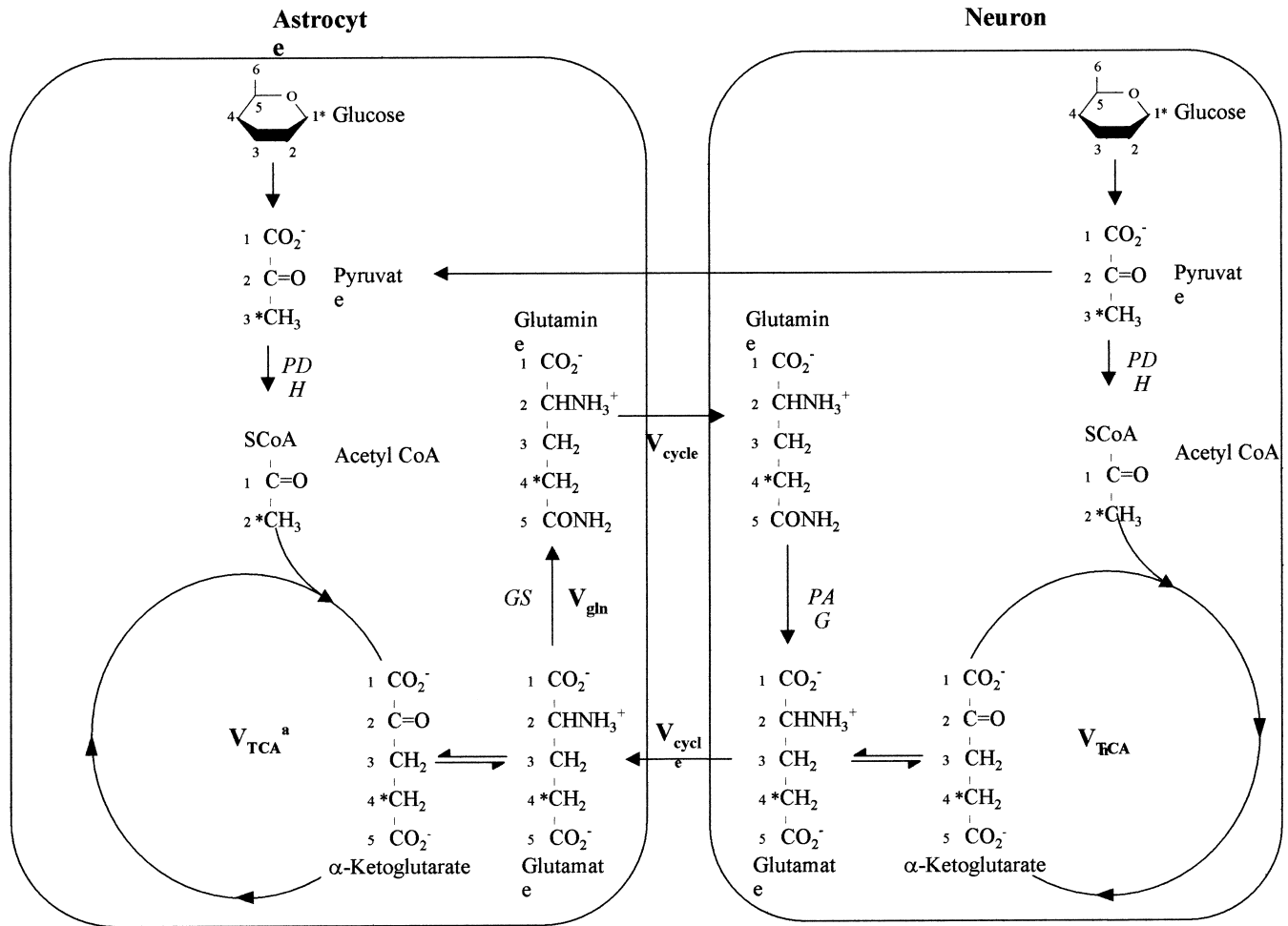


FIGURE 25.3. Isotopic labeling of C4-glutamine by the glutamate/glutamine cycle from a [1-¹³C] glucose precursor. Infused [1-¹³C] glucose labels neuronal C3-pyruvate. This label is then incorporated via the combined action of pyruvate dehydrogenase and the TCA cycle into α -ketoglutarate, which is in rapid exchange with glutamate due to the action of several transaminases. The large glutamate pool in the neuron acts as a label trap with [4-¹³C]-glutamate accumulating at the rate of the neuronal TCA cycle. Released [4-¹³C] glutamate from the nerve terminal is taken up by glial transport and the ¹³C label is transferred to [4-¹³C] glutamine through the action of glutamine synthetase at the rate of the glutamate/glutamine cycle. Interpretation of glutamine labeling is complicated by ¹³C label entering by the astrocyte pyruvate dehydrogenase reaction. MRS studies using ¹⁵N ammonia, [2-¹³C] glucose, and [2-¹³C] acetate, as well as comparison with traditional measurements of the uptake of net glutamine precursors, have shown that the majority of labeling in glutamine from [1-¹³C] glucose is from the glutamate/glutamine cycle (27,36–39).

study were analyzed with a metabolic model to determine the relative rates of glucose oxidation in the glutamate and GABA pool. Under conditions of α -chloralose anesthesia the rate of glucose oxidation in GABAergic neurons was estimated to be between 10% and 20% of total neuronal glucose oxidation. This value is similar to previous estimates obtained using isotopic methods and by inhibiting the degradative enzyme GABA transaminase (24). It should be noted that determination of the rate of GABA synthesis from isotopic methods depends on the assumption that the glutamate precursor pool for GABA is severalfold lower in

concentration than GABA, an assumption that is consistent with findings using cellular staining (41,42). In the recent studies of human cerebral cortex (13,29,35), the rate of GABA synthesis, and by inference glucose oxidation in the GABAergic pool, was estimated to be on the order of 10% of total glucose oxidation, although no rates were given. In the future, with the higher sensitivity available using inverse MRS methods in combination with the development of ultrahigh field magnets for human studies, measurements of the rate of glucose oxidation in GABAergic neurons should be possible in humans.

In Vivo MRS Measurements of the Rate of Glucose Oxidation in Glia

A long-term controversy in brain metabolism studies has been the rate of glucose oxidation in glial cells. Early estimates range from 10% to over 50% of glucose oxidation (49). MRS may be used to measure the rate of glial glucose oxidation based on the localization of the enzyme glutamine synthetase in the glia (50). This localization allows the rate of the glial TCA cycle to be calculated from the labeling of glutamine from glial glutamate. The most quantitative early findings were by Van den Berg and co-workers (40), who, using ^{14}C isotopic labeling strategies, assigned a rate to glial pyruvate dehydrogenase, which they referred to as the small glutamate pool, of 15% to 25% of total pyruvate dehydrogenase (neuronal + glial) activity. The pyruvate dehydrogenase rate is equal to the rate of complete glucose oxidation by the TCA cycle plus the rate of net glial anaplerosis. These measurements were performed using extract analysis of whole brains. Two recent ^{13}C MRS measurements of humans have measured glial pyruvate dehydrogenase as accounting for between 8% (29) and 15% (35) of total pyruvate dehydrogenase activity in the occipital parietal lobe. A limitation of these studies is that they did not measure the rate of the glial TCA cycle, only the pyruvate dehydrogenase step, and therefore the total oxidative energy produced in the glia was not calculated. In a preliminary study in human cerebral cortex using $[2-^{13}\text{C}]$ acetate, which is exclusively incorporated into the astrocyte (28), as a tracer Lebon et al. (38) found that the glial TCA cycle accounts for approximately 15% of total glucose oxidation.

Summary and Remaining Questions

In vivo MRS measurements of nonactivated cerebral cortex in rats and humans have found that from 60% to over 80% of glucose oxidation is associated with the large glutamate pool, reflecting primarily glutamatergic neurons. The remainder is primarily distributed between GABAergic neurons and glia. The development of new labeling strategies such as $[2-^{13}\text{C}]$ acetate and higher sensitivity MRS measurements should allow the contributions of these cell types to be more accurately determined. Within the error of the MRS measurements, and the contribution of glutamate pools in other neuronal classes to the glucose oxidation measurement, there may be up to 10% of total glucose oxidation available for other cell types such as dopaminergic and serotonergic nerve terminals. An objection that has been raised to these findings is the possibility that small highly metabolically active pools may be missed by the MRS method. Under nonstimulated conditions the good agreement of the MRS measurement with AV difference and PET measurements of total glucose consumption indicate that the contribution of these small pools is not large. MRS measurements of glucose metabolism during cortical activation will be re-

viewed below (see *In Vivo* MRS Measurements of Neuroenergetics During Functional Activation).

IN VIVO MRS MEASUREMENTS OF THE RATE OF THE GLUTAMATE/GLUTAMINE CYCLE: FINDINGS AND VALIDATION

The function of the glutamate/glutamine cycle is to prevent depletion of the nerve terminal glutamate pool by synaptic release. Glial cells have a high capacity for transporting glutamate from the synaptic cleft in order to maintain a low ECF (extracellular fluid) concentration of glutamate (50, 51). *In vivo* and *in vitro* studies indicate that glutamate released by the neuron is taken up by the glia and converted to glutamine by glutamine synthetase (53,54), an enzyme found exclusively in glia (52). Glutamine is transported from the glia into the ECF where it is taken up by neurons and converted back to glutamate through the action of phosphate-activated glutaminase (PAG) (55). Based on extensive data from isotopic labeling studies, immunohistochemical staining of cortical cells for specific enzymes, isolated cell, and tissue fractionation studies, it has been proposed that glutamate (as well as GABA) taken up by the glia from the synaptic cleft may be returned to the neuron in the form of glutamine (40,56–58). The generally accepted model of the glutamate/glutamine neurotransmitter cycle is shown in Fig. 25.1A.

Despite a wealth of evidence from enzyme localization and isolated cell studies, the rate of the glutamate/glutamine cycle and its importance for brain function have been controversial due to difficulties in performing measurements in the living brain. Because the neurotransmitter glutamate is packaged in vesicles (59,60), controversy has arisen about the fraction of glutamate actually involved in the cycle, leading to the concept of a small “transmitter” versus a large “metabolic” glutamate pool. Supporting the concept that glutamate neurotransmitter flux is a small fraction of total glucose metabolism are findings in isolated cells and nonactivated brain slices of a low rate of label incorporation from $[1-^{13}\text{C}]$ glucose (61). The concept of a metabolically inactive neurotransmitter pool was brought into question in 1995, when, using ^{13}C nuclear magnetic resonance (NMR), we measured a high rate of glutamine labeling from $[1-^{13}\text{C}]$ glucose in the occipital/parietal lobe of human subjects (12). A high rate of glutamine synthesis was calculated from these data (18). At the time of the initial ^{13}C NMR study, the rate of the glutamate/glutamine cycle could not be calculated due to the lack of a model for distinguishing isotopic labeling from this cycle from other sources of glutamine labeling, most significantly removal of cytosolic ammonia produced by metabolism and uptake of plasma ammonia (62). Net ammonia removal requires the *de novo* glutamine synthesis via the anaplerotic pathway in the glia. In addition, several other pathways, including the glial TCA cycle, have been proposed as providing significant precursors for gluta-

mine synthesis (61,62). To calculate the rate of the glutamate/glutamine cycle, Sibson et al. (25) developed a metabolic model for separating the pathways of glutamine synthesis.

This section reviews ^{13}C MRS measurements of the glutamate/glutamine cycle, emphasizing studies performed to validate the MRS technique. The important and surprising result of these studies is that the glutamate/glutamine cycle is a major metabolic flux, far exceeding de novo glutamine synthesis. The rate of the glutamate/glutamine cycle in the awake resting human cerebral cortex is between 60% and 80% of total glucose oxidation.

Development of a Two-Compartment Metabolic Model of Glutamine Metabolism to Separately Determine the Rate of the Glutamate/Glutamine Cycle and Anaplerotic Glutamine Synthesis

The rate of the glutamate/glutamine cycle is calculated from the time course ^{13}C labeling of glutamine relative to the labeling of its precursor neuronal glutamate. If neuronal glutamate were the only precursor of glutamine, the calculation would be straightforward. Unfortunately, the calculation is complicated by label from $[1-^{13}\text{C}]$ glucose entering both the neuronal and glial TCA cycles via pyruvate dehydrogenase. Glutamate in both cell types will be labeled in the C4 position by exchange with α -ketoglutarate in the TCA cycle (Fig. 25.3). The flow of label from C4-glutamate into C4-glutamine is proportional to the total rate of glutamine synthesis. However, unless the relative flow of ^{13}C label into the glial glutamate pool from the glial pyruvate dehydrogenase and neuronal glutamate are distinguished, the fraction of glutamine synthesis due to the glutamate/glutamine cycle cannot be calculated. To determine the rate of the glutamate/glutamine cycle from a $[1-^{13}\text{C}]$ glucose precursor, we developed a metabolic model to constrain the rate of glutamine labeling from glial pyruvate dehydrogenase.

Glutamine production via glutamine synthetase requires two substrates, glutamate and ammonia. As shown in the flow diagram of Fig. 25.1A, glutamine synthesis receives precursor glutamate from both glial uptake of released neurotransmitter glutamate and glial anaplerosis. A mathematical model was developed to interpret isotopic data in order to separate these pathways (25,27,29,36). The model extends previous formulations by imposing mass balance constraints on the brain glutamate and glutamine pools that relate the rate of de novo glutamine synthesis to the net uptake of anaplerotic precursors from the blood. Glutamine efflux is the primary source of nitrogen removal from the brain (49,62). Nitrogen must be removed from the brain in order to maintain low concentrations of ammonia, which when elevated will interfere with brain function (62). Because at steady state the concentration of glutamine remains

constant, loss of glutamine by efflux (V_{efflux}) must be compensated for by de novo synthesis of glutamine by anaplerosis (V_{ana}). For de novo synthesis by anaplerosis, pyruvate derived from glucose is converted by CO_2 fixation (V_{CO_2}) to oxaloacetate by the enzyme pyruvate carboxylase, which is active only in the glia (54). Through the action of the TCA cycle oxaloacetate is converted to α -ketoglutarate, which may be converted to glutamate either by ammonia fixation via glial glutamate dehydrogenase or alternatively through transamination with other amino acids (37). Glial glutamate is then converted to glutamine by glutamine synthetase. One or two ammonia molecules are fixed per glutamine molecule synthesized through anaplerosis, depending on the relative fluxes of NH_4^+ fixation versus transamination. Applying nitrogen mass balance constraints leads to the relationship $V_{\text{NH}_4} = (1 \text{ to } 2)V_{\text{efflux}}$ at steady state. The additional requirement of carbon mass balance leads to the following relationship:

$$V_{\text{ana}} = V_{\text{efflux}} = V_{\text{CO}_2} = (\frac{1}{2} \text{ to } 1)V_{\text{NH}_4} \quad [1]$$

Total glutamine synthesis is then related to synthesis for ammonia detoxification (V_{ana}) and the glutamate/glutamine cycle (V_{cycle}) by the following expression:

$$V_{\text{gln}} = V_{\text{cycle}} + V_{\text{ana}} \quad [2]$$

Note that V_{CO_2} may be higher than V_{ana} if anaplerosis is needed to replace TCA cycle intermediates lost by oxidative processes or pyruvate recycling (63,64).

Examination of Eq. 2 indicates that V_{cycle} may be derived from a measurement of V_{gln} from a ^{13}C MRS experiment in combination with a measurement of any of the rates linked by mass balance considerations to anaplerotic glutamine synthesis. A limitation of isotopic measurements of flux is that isotopic exchange cannot be distinguished from net flux. The linkage between the labeling of glutamine through glial pyruvate dehydrogenase and the brain anaplerosis flux allows the validation of isotopic measurements of glutamine ^{13}C and ^{15}N labeling against traditional AV difference measurements.

The glutamate/glutamine cycle measurement using a $[1-^{13}\text{C}]$ glucose precursor also includes contributions from the GABA/glutamine cycle (34,57,65). GABA is the main inhibitory neurotransmitter, and has been measured by *in vivo* ^1H and ^{13}C MRS in animals and humans (12,13,24,29,35,66) (see *In Vivo* MRS Studies of GABA Metabolism and the Effects of Disease and Pharmacologic Treatment on Human GABA Metabolism, below). The glutamate/glutamine and GABA/glutamine pathway may be distinguished using $[2-^{13}\text{C}]$ glucose and $[2-^{13}\text{C}]$ acetate as precursors as described below and in the section *In Vivo* MRS Studies of GABA Metabolism.

^{13}C NMR Studies of the Glutamate/Glutamine Cycle in Rat Cerebral Cortex

To determine the rate of glutamine synthesis, rats were studied under α -chloralose anesthesia in a 7-T modified Bruker

Biospec spectrometer. A small ^{13}C surface coil was used for transmission and reception. The spectroscopic volume was localized primarily to the motor and somatosensory cortices. The rats were infused with $[1-^{13}\text{C}]$ glucose, and the time course of label incorporation into the C4 positions of glutamate and glutamine was measured. The time courses were fitted using differential equations describing the proposed model of glutamate/glutamine cycle. The rate of the neuronal TCA cycle as measured from label incorporation into the C4-glutamate was $0.46 \pm 0.12 \mu\text{mol/g-min}$ [mean \pm standard deviation (SD), $n = 5$]. The rate of glutamine synthesis (V_{gln}) was $0.21 \pm 0.04 \mu\text{mol/g-min}$ ($n = 5$), which was nearly half the rate of the TCA cycle (25). These results indicate that glutamine synthesis is a major metabolic pathway in the rat cerebral cortex.

Validation of the Metabolic Model by Comparison of the Increase in the Rate of Glutamine Synthesis During Hyperammonemia with Independent Measures of Net Ammonia Uptake, CO_2 Uptake, and Glutamine Efflux

Elevated plasma ammonia increases the rate of the anaplerotic pathway of glutamine synthesis (62) in order to remove ammonia from the brain. The metabolic model predicts that under conditions of elevated plasma ammonia the increase in the rate glutamine synthesis is stoichiometrically coupled to the increase in the uptake of the anaplerotic substrates CO_2 and ammonia and the efflux of glutamine from the brain ($\Delta V_{\text{gln}} = \Delta V_{\text{ana}} = \Delta V_{\text{efflux}} = \Delta V_{\text{CO}_2} = \frac{1}{2}\Delta V_{\text{NH}_4\text{s}}$). To test the ^{13}C MRS measurement, glutamine synthesis in rat cerebral cortex was measured under normal and elevated plasma ammonia concentrations. Rats were made hyperammonemic ($0.35 \pm 0.08 \text{ mM}$ plasma ammonia vs. basal levels of $0.05 \pm 0.01 \text{ mM}$) by a primed continuous infusion of ammonia and studied after 4 hours of hyperammonemia to ensure metabolic steady state. The neuronal TCA cycle rate was not significantly increased under these conditions relative to the control condition, which suggests that brain electrical activity and by inference the glutamate/glutamine cycle were not substantially altered. The rate of glutamine synthesis under hyperammonemic conditions increased by $0.11 \pm 0.03 \mu\text{mol/g-min}$ relative to the rate under normal plasma ammonia levels. The increase in the rate of glutamine efflux (V_{efflux}) measured by AV difference under similar conditions was $0.10 \mu\text{mol/g-min}$ (67), in good agreement with ΔV_{gln} . Studies that have used ^{14}C isotope to measure the increase in V_{CO_2} with hyperammonemia found a rate of $\sim 0.15 \mu\text{mol/min-g}$ (68), which is slightly higher than measured by ^{13}C MRS, possibly due to the need for additional incorporation of CO_2 to replace TCA cycle intermediates lost by oxidation. As described below, both AV difference and direct isotope incorporation measurements of ammonia fixation into glu-

tamine under hyperammonemic conditions are also consistent with the predictions of the model. The agreement between the increase in V_{gln} determined by ^{13}C MRS and the increase measured by conventional methods in anaplerotic substrate utilization and glutamine efflux predicted by Eq. 2 provides strong experimental support for the ability to determine V_{cycle} under normal physiologic conditions.

^{15}N MRS Studies to Test the Relationship Between Anaplerotic Glutamine Synthesis and Ammonia Detoxification

^{15}N MRS is a useful method for both *in vitro* and *in vivo* study of cerebral glutamate/glutamine metabolism under hyperammonemic conditions based on the measurement of $[5-^{15}\text{N}]$ glutamine and $[2-^{15}\text{N}]$ glutamate/glutamine (69, 70). Incorporation of ^{15}N labeled ammonia into the N5 position of glutamine may be analyzed to calculate the flux through glutamine synthetase. In the absence of label exchange, the rate of incorporation of labeled ammonia into the N2 position of glutamate + glutamine may be analyzed to calculate the rate of glutamate dehydrogenase.

The relationships in Eq. 2, which were used in the modeling of the ^{13}C MRS data to deconvolute ^{13}C labeling in C4-glutamine from neuronal glutamate and glial PDH, are based on mass balance and previous AV difference and ammonia trapping studies. To further test the relationship of Eq. 2 between the rate of ammonia uptake in the cerebral cortex (V_{NH_4+}) and anaplerotic glutamine synthesis (V_{ana}), total ammonia uptake was calculated from the time course of the sum of ^{15}N labeled N5 glutamine and N2 glutamate + glutamine in rat cerebral cortex during infusion of ^{15}N ammonia. These were the only compounds into which appreciable ^{15}N label incorporation was observed, which agrees with previous findings that the major flows of ammonia in the brain involve these metabolites (62). The calculated V_{NH_4+} from these data was $0.13 \pm 0.02 \mu\text{mol/g-min}$ ($n = 6$). Based on the stoichiometric relationship of the model of $\frac{1}{2}\Delta V_{\text{NH}_4} = \Delta V_{\text{ana}}$, a rate of anaplerotic glutamine formation of $0.065 \pm 0.01 \mu\text{mol/g-min}$ was predicted. From this measurement an increase in the cerebral glutamine pool during the infusion of $0.065 \mu\text{mol/min/g} \times 180 \text{ min} = 11.7 \mu\text{mol/g}$ of glutamine was predicted. This calculation is in excellent agreement with the measured increase in glutamine concentration at the end of the study of $11.1 \pm 0.4 \mu\text{mol/g}$ (36).

^{13}C MRS Determination of the Rate of the Glutamate/Glutamine Neurotransmitter Cycle Under Normal Physiologic Conditions

To determine the rate of the glutamate/glutamine cycle from a $[1-^{13}\text{C}]$ glucose precursor under physiologic condi-

tions, Sibson et al. (25) measured V_{gln} and calculated V_{ana} using Eq. 2 and previously published measurements (62, 71). The value of V_{ana} calculated in this manner ranged from 0.00 to 0.04 $\mu\text{mol/g-min}$. Comparison with the ^{13}C MRS measurement of V_{gln} of $0.21 \pm 0.04 \mu\text{mol/g-min}$, yields a V_{cycle} that is 80% to 90% of the rate of glutamine synthesis. A similar high percentage of V_{cycle} was calculated using measurements of the net incorporation of $^{14}\text{CO}_2$ into the cerebral cortex (72). The CO_2 measurement is coupled to total brain anaplerosis, which may be higher than anaplerosis used for net glutamine synthesis, and therefore represents the maximum estimate of this flux.

Validation of the Measurement of Glutamine Synthesis by Comparison of Rates Calculated from ^{15}N MRS and ^{13}C MRS Results

To obtain an independent measurement of V_{gln} and V_{ana} , ^{15}N MRS was used to measure the rate of ^{15}N -labeled ammonia incorporation into the N5 position of glutamine and the unresolved resonance of N2 glutamate plus glutamine (36). A mathematical analysis based on the model was used to derive V_{gln} from the MRS measurement of the time course of $[5\text{-}^{15}\text{N}]$ glutamine and $[2\text{-}^{15}\text{N}]$ glutamate + glutamine. The labeling in the first hour was almost exclusively within the N5 position of glutamine, which is consistent with the delayed onset of anaplerosis previously reported under these conditions (73) and previous measurements using ^{13}N and ^{15}N labeled ammonia (62,69). The low initial rate of anaplerosis allows the rates determined from the ^{15}N NMR study to be compared with the rates measured by ^{13}C NMR under normal physiologic conditions. The measured V_{gln} of $0.20 \pm 0.06 \mu\text{mol/g-min}$ (mean \pm SD, $n = 6$) from these studies (36) is in excellent agreement with the results from the ^{13}C NMR measurement of $0.21 \pm 0.04 \mu\text{mol/g-min}$ (25).

Validation of the ^{13}C MRS Measurement of the Glutamate/Glutamine Cycle, and Assessment of Alternate Models of Neuronal/Glial Trafficking, Through Comparison of Results Using $[1\text{-}^{13}\text{C}]$ Glucose, $[2\text{-}^{13}\text{C}]$ Glucose, $^{15}\text{NH}_4$, and $[2\text{-}^{13}\text{C}]$ Acetate as Precursors

Several alternative models to the glutamate/glutamine cycle (Fig 25.1A,B) have been proposed. In one alternative model the ^{13}C labeling of glutamine represents an internal glial glutamate/glutamine cycle as opposed to trafficking between the neuron and glia. Label enters C4-glutamine from $[1\text{-}^{13}\text{C}]$ glucose in this model through exchange in the glial cell between glutamate and glutamine catalyzed either through the reverse reaction of glutamine synthetase, or al-

ternatively via glial phosphate activated glutaminase. Released neuronal glutamate in this model is taken up directly by the nerve terminal. In another alternate model, diagrammed in Fig. 25.1C, the glia releases α -ketoglutarate, or equivalently citrate or malate, to the neuron to replace the carbon skeleton of released glutamate (32,34,64). In support of this pathway, which is referred to here as the glutamate/ α -ketoglutarate cycle, several TCA cycle intermediates including malate, α -ketoglutarate, and citrate are released from glia in cell culture and may be taken up by synaptosomes and cultured neurons (32–34).

The two pathways of glutamate trafficking shown in Fig. 25.1 cannot be distinguished on the basis of a ^{13}C MRS study using $[1\text{-}^{13}\text{C}]$ glucose as the label source. As described above, $[1\text{-}^{13}\text{C}]$ glucose will label both the glial and neuronal glutamate pools directly via pyruvate dehydrogenase. An alternative strategy is to use isotopic precursors that exclusively introduce label into the glia. Analysis of the flow of isotope from the glia into the neuronal glutamate pool yields the rate of total neuronal/glial glutamate trafficking. Comparison with the rate calculated using $[1\text{-}^{13}\text{C}]$ glucose gives the fraction of neuronal/glutamate trafficking due to the glutamate/glutamine cycle (27,36).

The initial use with MRS of the strategy of glial selective precursors to calculate the fraction of glutamate trafficking due to the glutamate/glutamine cycle measurement was by Shen et al. (36), who calculated the relative fraction of the glutamate/glutamine cycle and glutamate/ α -ketoglutarate cycle, using ^{15}N MRS measurement of the labeling in glutamine and glutamate from $^{15}\text{NH}_4^+$. Under hyperammonemic conditions the rate of ^{15}N ammonia incorporation into the N5 and N2 position of glutamine is the same in the glutamate/ α -ketoglutarate cycle because only the anaplerotic pathway of glutamine synthesis is present. In contrast, in the glutamate/glutamine cycle, there is additional incorporation of ^{15}N label into the N5 position of glutamine selectively in the glia (due to the localization of glutamine synthetase) due to the cycle. To distinguish these models, the endpoint ^{15}N enrichment of the N2 positions of glutamate and glutamine were calculated relative to the glutamine N5 position for each model using the N5 glutamine labeling curve as an input and compared with experimental values. As shown in Fig. 25.4, the low ^{15}N fractional enrichment of the N2 position of glutamine and glutamate relative to glutamine N5 at the end of the study strongly supports the glutamate/glutamine cycle as the primary pathway of neuronal glutamate repletion.

An additional test of the glutamate/glutamine cycle model was recently performed using $2\text{-}^{13}\text{C}]$ glucose as an isotopic precursor (27). Label from $[2\text{-}^{13}\text{C}]$ glucose enters the inner positions of glutamate and glutamine only through pyruvate incorporation into the TCA cycle by pyruvate carboxylase, which is localized to the glia (27,74). The initial flow of label from this precursor is into the glial TCA cycle intermediates, and then glial glutamate and glu-

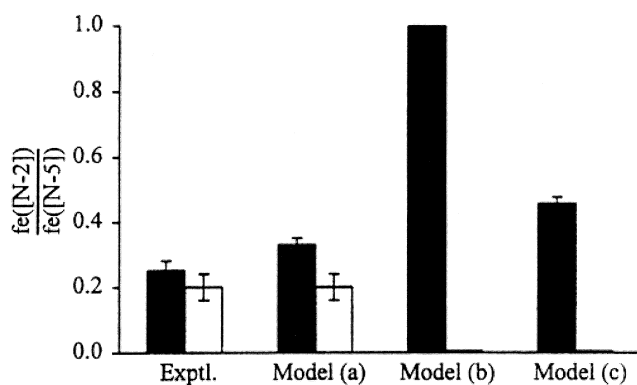


FIGURE 25.4. Calculated $^{15}\text{N}_2/^{15}\text{N}_5$ fractional enrichment ratios of glutamine and glutamate for three models of glial glutamine synthesis. Three models of neuronal glutamate completion were compared with experimental results in which the time course of $[5-^{15}\text{N}]$ glutamine and $[2-^{15}\text{N}]$ glutamine and glutamate were measured by ^{15}N nuclear magnetic resonance (NMR) in the cortex of a rat infused with ^{15}N -labeled ammonia at 7 T (36). The measured ratio at the end of the infusion is in excellent agreement with the ratio predicted if the glutamate/glutamine cycle is the major pathway of astrocytic repletion of released neuronal glutamate (model a, which is diagrammed in Fig 25.1A,B). If instead the cycle was internal to the astrocyte the N_2/N_5 glutamine relative ^{15}N enrichment would be two times higher than measured and no labeling would have been observed in N_2 glutamate (model b). If glutamate neurotransmitter repletion took place through the astrocytes providing the neurons with α -ketoglutarate (model c, which is diagrammed in Fig 25.1C), the rate of anaplerotic and total glutamine synthesis would be similar and the N_5/N_2 ratio of glutamine would be close to 1.0 as opposed to the measured ratio of 0.25. A similar labeling strategy has recently been used with $[2-^{13}\text{C}]$ glucose and $[2-^{13}\text{C}]$ acetate, both substrates that selectively label glutamine through glial specific pathways, and has put an upper limit of the rate of the α -ketoglutarate/glutamate cycle at 20% of the total rate of glutamate trafficking, the remainder being due to the glutamate/glutamine cycle (27,38).

tamine (27). Subsequently, neuronal/glial cycling moves the label to the neuron where it labels the large glutamate pool. The labeling measured in the glutamate pool is the sum of all trafficking pathways from the glia. In contrast the rate of labeling of glutamine from a $[1-^{13}\text{C}]$ glucose precursor is a measure of the glutamate/glutamine cycle. *In vivo* and *in vitro* ^{13}C MRS at 7 T was recently used to measure the labeling time course of glutamate and glutamine in the cerebral cortex of rats under hyperammonemic and normoammonemic conditions during infusion of either $[1-^{13}\text{C}]$ or $[2-^{13}\text{C}]$ glucose (27). The rate calculated for the neuronal/glial glutamate cycle was similar, with both labels indicating that the glutamate/glutamine cycle is the major pathway of neuronal/glial glutamate trafficking accounting for between 80% and 100% of total glutamate trafficking. A similar conclusion was recently reported for human cerebral cortex using $[2-^{13}\text{C}]$ acetate as a precursor (38), which selectively introduces label into glutamate and glutamine through glial pyruvate dehydrogenase.

The Effect of Glutamate Oxidation on the Glutamate/Glutamine Cycle Measurement and Estimates of Its Rate *In Vivo*

An alternate pathway of neuronal/glial glutamate trafficking is glial glutamate oxidation (10,63,64). In this pathway glutamate taken up by the glial cell is transaminated into α -ketoglutarate and enters the TCA cycle. Reactions in the TCA cycle convert α -ketoglutarate to oxaloacetate, which is then converted to pyruvate by the action of malic enzyme. The pyruvate formed from glutamate is oxidized in the TCA cycle through the action of pyruvate dehydrogenase. Glutamate lost to the brain by this pathway is then replaced by anaplerosis through pyruvate carboxylase. Evidence of this pathway is derived primarily from isolated cell cultures. It has been proposed that the fraction of glutamate going through this pathway increases with brain electrical activity (64).

The major effect of the glutamate oxidation pathway on the MRS measurement of the glutamate/glutamine cycle is to cause the fraction of glutamine synthesis of net anaplerosis to be overestimated and V_{cycle} to be consequently underestimated, because the labeling of the internal positions of glutamine from the two pathways from $[1-^{13}\text{C}]$ and $[2-^{13}\text{C}]$ glucose is similar. The unambiguous *in vivo* determination of glutamate oxidation requires the ^{13}C label flow from glutamate to pyruvate to be measured (10,63). This measurement is complicated by other metabolic pathways that produce similar labeling patterns, including scrambling of isotopic labeling into other positions of glucose in the liver (23,27,63,75), and as a consequence glutamate oxidation has not been definitively demonstrated *in vivo* under normal physiologic conditions. Suggestive evidence of this pathway is the finding in several studies that the rate of anaplerosis under normal ammonia conditions calculated from labeling of glutamine by ^{13}C labeled glucose is approximately two to three times higher than that predicted from measurements of brain glutamine efflux (27). An alternate possibility is that rather than glutamate oxidation this extra labeling reflects cycling between oxaloacetate and pyruvate to generate reduced nicotinamide adenine dinucleotide phosphate (NADPH) reducing equivalents in the glia, a pathway that has been shown to be highly active in the liver (75).

Validation of the ^{13}C MRS Glutamate/Glutamine Cycle Measurement by Correlation with Brain Electrical Activity

If the ^{13}C labeling measured in glutamine by ^{13}C MRS is due to the glutamate/glutamine cycle, then the calculated rate of this pathway should correlate with brain electrical activity. Neuronal glutamate release is known to increase with neuronal depolarization associated with action poten-

tials. To test this prediction, ^{13}C MRS was used to measure the rates of neuronal glucose oxidation and the glutamate/glutamine cycle in the rat cerebral cortex at three levels of cortical electrical activity: isoelectric EEG induced by high-dose pentobarbital anesthesia, and at two milder levels of anesthesia (26). During isoelectric conditions, under which minimal glutamate release takes place, almost no glutamine synthesis was measured, consistent with the conclusion that the ^{13}C MRS measurement of glutamine synthesis primarily reflects the glutamate/glutamine cycle. Above isoelectricity, the rates of the glutamate/glutamine cycle and neuronal glucose oxidation both increased with higher electrical activity. The relationship measured in this study between the rate of the glutamate/glutamine cycle and neuronal glucose oxidation is described below (see Determination of the *In Vivo* Coupling Between the Rate of the Glutamate/Glutamine Neurotransmitter Cycle and Neuronal Glucose Oxidation).

^{13}C MRS Measurements of the Rate of the Glutamate/Glutamine Cycle in Human Cerebral Cortex

In 1994 we first demonstrated that *in vivo* ^{13}C NMR may be used to measure the rate of glutamine labeling (12,18) from $[1-^{13}\text{C}]$ glucose in human occipital/parietal cortex. These studies showed clearly that glutamine is labeled rapidly from $[1-^{13}\text{C}]$ glucose in the human cerebral cortex. However, the rate of the glutamate/glutamine cycle was not uniquely determined in the initial experiments due to the inability to distinguish the glutamate/glutamine cycle from other sources of glutamine labeling. To determine whether there is a similar high rate of the glutamate/glutamine cycle in human cerebral cortex as in the rat, we (29) and Gruetter and co-workers (13,35) have determined this rate from ^{13}C MRS measurements in the human occipital/parietal lobe.

A time course from the study of Shen and co-workers (29) showing the rapid labeling of C4-glutamine and C4-glutamate from $[1-^{13}\text{C}]$ glucose in a single subject is shown in Fig. 25.5. A best fit of the metabolic model is plotted through the data. A lag is clearly shown in the labeling of C4-glutamine relative to C4-glutamate, which is consistent with the large neuronal glutamate pool being the main precursor for glutamine synthesis. The combination of the metabolic model validated in the rodent and improved MRS sensitivity allowed the rate of the glutamate/glutamine cycle, the neuronal TCA cycle, the glial TCA cycle, and anaplerotic glutamine synthesis to be calculated from the ^{13}C MRS data. The analysis gave a total TCA cycle rate of $0.77 \pm 0.05 \mu\text{mol}/\text{min}/\text{g}$ (mean \pm SD, $n = 6$), a neuronal TCA cycle rate of $0.71 \pm 0.02 \mu\text{mol}/\text{min}/\text{g}$, a glial TCA cycle rate of $0.06 \pm 0.02 \mu\text{mol}/\text{min}/\text{g}$, a glutamate-glutamine cycle rate of $0.32 \pm 0.04 \mu\text{mol}/\text{min}/\text{g}$ (mean \pm SD, $n = 6$), an anaplerotic glutamine synthesis rate of 0.04 ± 0.02 , and a glucose oxidation rate of $0.39 \pm 0.03 \mu\text{mol}/\text{min}/\text{g}$

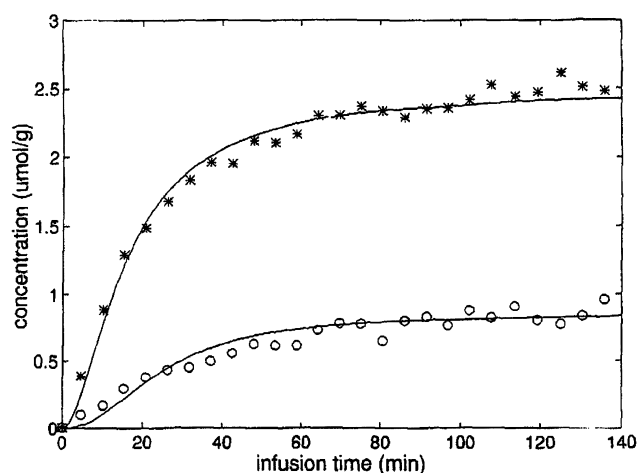


FIGURE 25.5. *In vivo* ^{13}C NMR time course of the human occipital/parietal lobe: the time course from one subject of the concentrations of $[4-^{13}\text{C}]$ glutamate and $[4-^{13}\text{C}]$ glutamine during a $[1-^{13}\text{C}]$ glucose infusion, and the best fit of the two-compartment model to these data. At time 0 on the plot an intravenous infusion of $[1-^{13}\text{C}]$ glucose was started. The model is shown to provide an excellent fit to the data. The rise of $[4-^{13}\text{C}]$ glutamine is clearly seen to lag the labeling of $[4-^{13}\text{C}]$ glutamate, consistent with neuronal glutamate being the main precursor for glutamine synthesis via the glutamate/GABA/glutamine cycle. *, glutamate; o, glutamine. (From Shen J, Petersen KF, Behar KL, et al. Determination of the rate of the glutamate-glutamine cycle in the human brain by *in vivo* ^{13}C NMR. *Proc Natl Acad Sci USA* 1999;96:8235–8240, with permission.)

(mean \pm SD, $n = 6$). In agreement with studies in rat cortex, the glutamate/glutamine cycle is a major metabolic flux in the resting human brain with a rate approximately 80% of the rate of total glucose oxidation.

In a study performed at 4 T, Gruetter and co-workers (13) measured rapid labeling of glutamate and glutamine from infused $[1-^{13}\text{C}]$ glucose using ^{13}C MRS. A high rate of the glutamate/glutamine cycle was measured using a two-compartment model, similar to the model used by Shen and co-workers (29). The improved spectroscopic resolution provided by the higher field strength at 4 T allowed the additional positions of the C2 and C3 resonances of aspartate, glutamate, and glutamine to be incorporated into the modeling. More recently Gruetter and co-workers (35) studied six subjects using localized ^{13}C MRS measurements of a 45-mL volume in the occipital lobe. The main differences from the rates derived from the Shen et al. (29) study are a higher rate of anaplerosis, approximately 25% of total glutamine synthesis as opposed to 11% in the Shen et al. study and a somewhat lower rate of the neuronal TCA cycle of $0.62 \pm 0.05 \mu\text{mol}/\text{min}/\text{g}$. The lower calculated neuronal TCA cycle rate was due to a lower rate of neuronal mitochondrial α -ketoglutarate/glutamate exchange calculated from the data than in a previous study by Mason and co-workers (18). The lower exchange rate was due to the assignment of a higher concentration of aspartate in the gluta-

matergic neuron and glutamate in the astrocyte in the metabolic model of Gruetter and co-workers. The higher anaplerosis rate also reflects differences in which the isotopic data was modeled. In the Shen et al. study anaplerosis was calculated primarily from the labeling kinetics of C4-glutamine and C4-glutamate, whereas in the Gruetter et al. (35) study it was calculated primarily from the measurement of the time course of the differential ^{13}C labeling of the C2, C3, and C4 glutamate and glutamine resonances. Both approaches suffer from needing to deconvolute ^{13}C label entering these carbon positions from pyruvate dehydrogenase from the label entering via pyruvate carboxylase. In the future these differences should be reconcilable by using labeling strategies such as [2- ^{13}C] glucose, which labels glutamate and glutamine internal positions only by pyruvate carboxylase. If the anaplerotic pathway is due to glutamate oxidation (see Validation of the ^{13}C MRS Glutamate/Glutamine Cycle Measurement by Correlation with Brain Electrical Activity, above) as opposed to ammonia detoxification, the rate of the glutamate/glutamine cycle reported in both studies is an underestimate by the calculated rate of anaplerosis. The differences in the anaplerotic flux calculated in these studies should not obscure the major point of agreement—that the glutamate/glutamine cycle is major metabolic pathway with a rate accounting for between 60% and 80% of total glucose oxidation in the cerebral cortex.

Cellular and Molecular Evidence that Astroglia have a Major Role in the Uptake of Glutamate Released from Neurons

The high rate of the glutamate/glutamine cycle indicates that astroglial uptake of glutamate and GABA plays a key role in maintaining the low extracellular levels of these neurotransmitters needed for proper receptor-mediated functions. There is considerable evidence from several lines of research that support this conclusion. Overstimulation of glutamate receptors can lead to excitotoxicity (76,77). Studies of glutamatergic synapses have shown them to be closely surrounded by glial end processes possessing high densities of glutamate transporters (78). Glutamate and GABA transporters are sodium dependent and electrogenic and are present on both neurons and glia (58,78–80). Glutamate transporters have an affinity, K_m , of 1 to 3 μM (80), which is in the range of normal estimated ECF glutamate concentrations. Immunohistochemical studies have showed that the glutamate transporters GLT-1 and GLAST (glutamate astrocytic transporter) are localized primarily in astrocytes (48, 81–83), whereas EAAC1 is found on neurons (51). Antisense oligonucleotides directed against the astrocytic glutamate transporters GLT-1 or GLAST *in vivo* results in elevated ECF glutamate *in vivo* and excitotoxicity (84,85). The majority of glutamate uptake after its release appears to be either postsynaptic or astroglial (86,87), although an elec-

trophysiologic study of the hippocampal slice suggests that astroglial uptake dominates (88).

Summary and Remaining Questions

MRS allows the glutamate/glutamine cycle to be measured from the labeling of glutamate and glutamine by ^{13}C and ^{15}N labeled precursors. The major complications in determining the rate of the glutamate/glutamine cycle from isotopic measurements are separating the labeling of glutamine from the glutamate/glutamine cycle from alternate pathways of glutamine synthesis and isotopic exchange, and distinguishing different pathways of neuronal/glial glutamate trafficking. To overcome these obstacles the metabolic modeling of the glutamate/glutamine cycle has been extended to include ammonia detoxification, alternate pathways of glutamate trafficking, and glutamate oxidation (27). The MRS rate measurement has been validated by several strategies including (a) comparison of the rate of glutamine synthesis measured under different ammonia levels with measurements of anaplerotic substrates by AV difference and isotopic trapping methods (25); (b) comparison of the rates of glutamine synthesis and the glutamate/glutamine cycle calculated from the isotopic labeling from [1- ^{13}C] glucose, [2- ^{13}C] glucose, ^{15}N ammonia, and [2- ^{13}C] acetate (27,35, 36,39); and (c) measurement of the rate of the glutamate/glutamine cycle as a function of brain electrical activity (26, 37). The results of these studies indicate that the glutamate/glutamine cycle is the major pathway of glutamine synthesis and neuronal/glial glutamate trafficking under normal conditions, with a rate similar to the rate of neuronal glucose oxidation under conditions of high electrical activity. Measurements in awake nonstimulated human cerebral cortex have found that the rate of the glutamate/glutamine cycle is between 60% and 80% of total glucose oxidative metabolism (29,35).

Objections have been raised to the MRS measurement of the glutamate/glutamine cycle for having neglected alternate pathways of glutamate trafficking and the need for comparison with direct measurements of neuronal glutamate release. As described above, isotopic strategies have been developed to assess these pathways and under physiologic conditions they were found to account for less than 20% of glutamate trafficking. However, under pathologic conditions such as seizure the rate of these pathways may be much higher. Glutamate oxidation may have a significant contribution to total neuronal/glial glutamate trafficking. However, the unambiguous *in vivo* measurement of glutamate oxidation will require strategies for eliminating isotopic labeling from other pathways. Although direct measurement of bulk neuronal release of glutamate for comparison with ^{13}C MRS is presently not possible, advances in molecular and cellular methods for studying glutamate transport indicate that neurotransmission is the major, if not exclusive, pathway of glutamate release from glutamatergic neurons and the vast

majority of this flux is taken up by astroglia in the cerebral cortex. Correlation of the MRS glutamate/glutamine cycle with indirect measures of neuronal glutamate release such as microdialysis and nerve terminal labeling would be highly desirable, as would further studies better defining the relevant pool sizes and enzyme distribution in glia and glutamatergic neurons, particularly in regions other than the cerebral cortex.

DETERMINATION OF THE *IN VIVO* COUPLING BETWEEN THE RATE OF THE GLUTAMATE/GLUTAMINE NEUROTRANSMITTER CYCLE AND NEURONAL GLUCOSE OXIDATION

This section presents evidence from MRS and other studies for a model of the coupling between the glutamate/glutamine cycle and glial glucose uptake and subsequent neuronal oxidation. The model is based on work in cellular systems primarily by Magistretti and co-workers (90) and recent findings, using ^{13}C MRS in rat cortex, that the glutamate/glutamine cycle (a) increases in rate with increasing brain electrical activity in a near 1:1 stoichiometry with neuronal glucose oxidation (26), and (b) is 60% to 80% of the rate of total glucose oxidation in the awake nonstimulated cerebral cortex (13,26,29,35,37). Several comprehensive reviews of the evidence from molecular and cellular studies supporting glial localization of glucose uptake related to functional neuroenergetics have been published by Magistretti and co-workers (52,89) and are not duplicated here. The focus of this section is on the evidence from *in vivo* studies that support the model and key tests that remain to be performed.

Determination by ^{13}C MRS of the Relationship Between the Glutamate/Glutamine Cycle and Neuronal Oxidative Glucose Consumption

To determine the relationship between the glutamate/glutamine cycle and cerebral cortex neuroenergetics, ^{13}C MRS was used to measure the rate of neuronal glucose oxidation and the glutamate/glutamine cycle in rat cortex under conditions of isoelectric EEG induced by high-dose pentobarbital anesthesia, and at two milder levels of anesthesia (26). The rate of neuronal glucose oxidation and the glutamate/glutamine cycle was calculated using a two-compartment metabolic model from the isotopic turnover of C4-glutamate and C4-glutamine. Under isoelectric conditions, at which minimal glutamate release takes place, almost no glutamine synthesis was measured, consistent with the conclusion that the ^{13}C MRS measurement of glutamine synthesis primarily reflects the glutamate/glutamine cycle. Above isoelectricity, the rates of the glutamate/glutamine cycle and

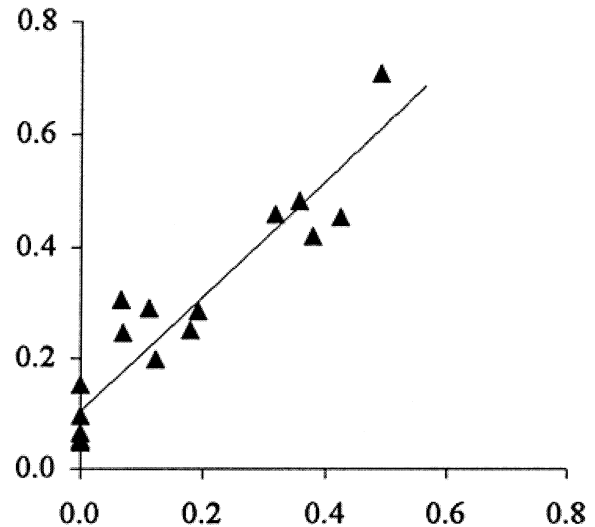


FIGURE 25.6. An approximately 1:1 correlation between the rate of oxidative glucose consumption and the rate of the glutamate glutamine cycle. The rate of neuronal glucose oxidation ($\text{CMR}_{\text{glc(ox)}}$) and the glutamate/glutamine cycle (V_{cycle}) was measured by ^{13}C MRS at 7 T in the rat somatosensory cortex at different levels of cortical activity induced by anesthesia. A significant positive correlation ($p < .001$) was found between $\text{CMR}_{\text{glc(ox)}}$ and V_{cycle} . The regression line shown is $y = 1.04x + 0.10$ with a Pearson product-moment correlation coefficient, r , of 0.94. (From Sibson NR, Dhankhar A, Mason GF, et al. Stoichiometric coupling of brain glucose metabolism and glutamatergic neuronal activity. *Proc Natl Acad Sci USA* 1998;95:316–321, with permission.)

neuronal glucose oxidation both increased with increasing electrical activity. The results, shown in Fig 25.6, indicate an approximately 1:1 relationship between the increase in the rates of the glutamate/glutamine cycle and neuronal glucose oxidation with brain activity. Under the highest cortical activity studied, the glutamate/glutamine cycle rate was approximately 80% of the rate of neuronal glucose oxidation. A similar ratio of the rate of the glutamate/glutamine cycle to the rate of neuronal glucose oxidation has been reported for measurements of awake nonstimulated human cerebral cortex (13,29,35).

A Model for the Stoichiometric Coupling of the Glutamate/Glutamine Cycle to Neuronal Glucose Oxidation

Figure 25.7 shows a model that provides a mechanistic explanation for the observed ratio of the rates of the glutamate/glutamine cycle to neuronal glucose oxidation (26,37,90). The model is an extension of the model proposed by Magistretti and co-workers that nonoxidative glial glycolysis is coupled to glutamate uptake due to the preference of the glia to use glycolytic adenosine triphosphate (ATP) to pump out the cotransported three Na^+ ions (52,90,91). The pyruvate and lactate formed by glial glycolysis would then be transported to the neuron where it is oxidized. Prior to the

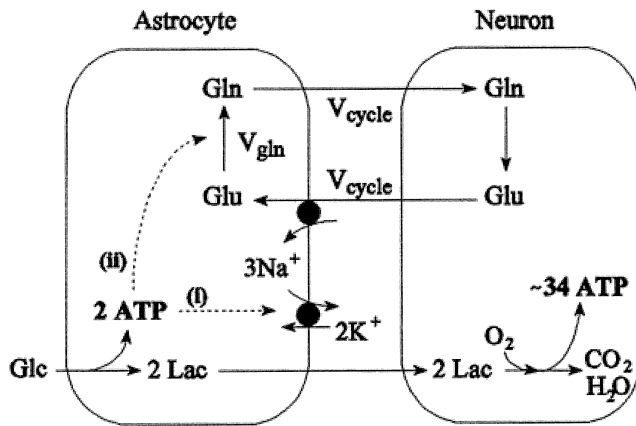


FIGURE 25.7. A metabolic model coupling the glutamate/glutamine cycle to oxidative glucose consumption. In this model the two molecules of adenosine triphosphate (ATP) required by the astrocyte to take up one molecule of glutamate (Glu) and convert it through glutamine synthetase to glutamine (Gln) are provided by nonoxidative glycolysis of one molecule of glucose (Glc). The lactate produced by nonoxidative glycolysis is then released from the astrocyte and taken up by the neuron for oxidative glycolysis. Glc, glucose; Lac, lactate; V_{gln} , rate of glutamine synthesis; V_{cycle} , rate of the glutamate/glutamine cycle. (From Sibson NR, Dhanekar A, Mason GF, et al. Stoichiometric coupling of brain glucose metabolism and glutamatergic neuronal activity. *Proc Natl Acad Sci USA* 1998;95:316–321, with permission.)

in vivo ¹³C MRS studies, the evidence for the model was primarily from enzyme localization studies and isolated cell studies (see refs. 89 and 90 for reviews of these studies). Both lines of evidence of localization have been criticized based on the presence of the enzymes required for glucose transport and glycolysis in the neurons, and the strong dependence of glutamate-stimulated glial glucose metabolism on cell culture conditions (92).

Comparison of the *In Vivo* ¹³C MRS Results with the Stoichiometry Predicted by the Model

The ambiguities in the determination of the relative rates of metabolic pathways from enzymatic localization and measurements of isolated cells are not unexpected. Metabolic control analysis has shown that the total activity of an enzyme within a metabolic pathway does not determine the flux through the pathway (93). Extrapolation to *in vivo* rates from studies of cell cultures is complicated by the difficulty of reproducing the complex cellular interactions that occur *in vivo* (64). To compare the results of the *in vivo* measurement with the predictions of the model, Sibson et al. (26) calculated the stoichiometric relationship between the glutamate/glutamine cycle and neuronal oxidative glucose consumption. Glutamate is cotransported into the glia with two to three Na⁺ ions, with one K⁺ ion countertransported (60,78,94). Transport of three Na⁺ ions out of the

glia by the Na⁺/K⁺ adenosine triphosphatase (ATPase) on the glial end process membrane requires approximately one ATP molecule (91). Synthesis of glutamine from glutamate through glutamine synthetase requires one ATP molecule per glutamine molecule synthesized (53). If the ATP for this process were derived entirely from glycolysis, then a 1:1 stoichiometry is predicted between glial nonoxidative glucose consumption and the glutamate/glutamine neurotransmitter cycle. Provided that the lactate formed is released to the neurons for oxidation, then this predicted stoichiometry is in excellent agreement with the *in vivo* ¹³C MRS findings.

If the model is correct, it may account for a substantial fraction of total glucose consumption in the awake nonstimulated cerebral cortex. Based on the measurements of the rate of the glutamate/glutamine cycle and total glucose oxidation in human cerebral cortex (13,29), between 60% and 80% of total brain glucose oxidation may be accounted for by this mechanism.

Additional *In Vivo* Evidence of the Model

The model (90) has been criticized for not leaving room for other energy consuming processes in the cerebral cortex. Within the error of the measurements, approximately 10% of total glucose oxidation is available for other neuronal systems such as dopaminergic or serotonergic. The finding of the large majority of glucose oxidation in the cerebral cortex being associated with glutamatergic and GABAergic neurons and their surrounding astrocytes is not surprising, because cell staining studies have shown that the vast majority of synapses and neurons in the cerebral cortex are either glutamatergic or GABAergic (4).

A prediction of the model is that a large fraction of glucose uptake and phosphorylation is localized in the cerebral cortex to the glial end sheaths surrounding the synapses of glutamatergic neurons. In agreement with this prediction studies using ¹⁴C-deoxyglucose autoradiography indicate that the majority of brain glucose uptake is used to support synaptic activity. Increased glucose uptake in response to functional stimulation in peripheral neurons and in cortex is primarily localized in dendritic and nerve terminal cortical layers (where there are associated glial end processes) and not in layers associated with cell bodies (1,95–97).

The rapid incorporation of ¹³C label into glutamine by the glutamate/glutamine cycle indicates that the vesicular glutamate pool is rapidly turning over and is in dynamic equilibrium with cytosolic glutamate. This conclusion is in contradiction to the traditional view that the small vesicular pool is metabolically isolated from cellular glutamate metabolism (60,61). However, these studies were performed in cellular and tissue preparations, which have a low rate of synaptic metabolism relative to intact cerebral cortex. In support of this conclusion Conti and Minelli (42) showed that inhibition of PAG, which is enriched in nerve terminals

(55) and has been proposed to primarily replete the vesicular pool of glutamate (34), results in a similar rapid depletion of both synaptic and whole cell glutamate in the rat cerebral cortex.

Further support for the coupling between glial glycolysis and the glutamate/glutamine cycle is provided from studies performed looking at glutamine synthesis in mice in which the astrocytic TCA cycle was inhibited by injection with fluoroacetate (28). In these studies mice were given fluoroacetate and injected with a combination of [1,2-¹³C] acetate and [1-¹³C] glucose. From measurements of the isotopomer distribution in glutamate and glutamine, the labeling from glucose and acetate was distinguished. The labeling from acetate in glutamate and glutamine was greatly reduced by fluoroacetate administration, which the authors interpreted as resulting from the near-complete inhibition of the glial TCA cycle. Despite this inhibition, there was still a substantial amount of glutamine labeling from [1-¹³C] glucose, approximately one-third to one-half the labeling found in the control mice. The only mechanism by which this labeling of glutamine from glucose could occur is the glutamate/glutamine cycle, because glutamate labeling in the astrocyte from glucose was completely blocked. The ability to maintain a high glutamate/glutamine cycle flux, despite the near-complete inhibition of glial mitochondrial ATP generation, has been interpreted by Bachelard (98) as supporting the importance of the glutamate/glutamine cycle as well as the potential coupling to glycolytic ATP production: "This singlet labeling of the C4 of glutamine, which can only be derived from [1-¹³C] glucose metabolism in the neurones, also quite clearly demonstrates that even though the glial TCA cycle is blocked by the toxin, the glia are still capable of participating in the glutamate-glutamine cycle, taking up glutamate from the neurones and converting it to glutamine."

Another testable prediction of the model is that if another substrate is supplied for neuronal oxidation, the decrease in glucose oxidation will be greater than the decrease in glucose consumption, due to the remaining need for glycolytic ATP to fuel the clearance of glutamate. Consistent with this prediction, an AV difference study of the anesthetized rat brain found that infusion of β -hydroxybutyrate, which is an alternate fuel for brain oxidative ATP production, led to a two- to threefold greater decrease in glucose oxidation than in glucose consumption, with the difference accounted for by a large increase in the efflux of lactate from the brain (99). Consistent with this finding, Pan et al. (100) measured an increase in brain lactate in 3-day-fasted human subjects with elevated plasma ketone concentrations,

Summary and Remaining Questions

The linear relationship and stoichiometry found using ¹³C MRS of the rates of the glutamate/glutamine cycle and neuronal glucose oxidation support a direct mechanistic coup-

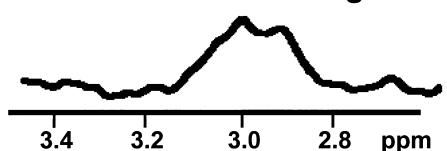
ling between the glutamate/glutamine cycle and glial glucose uptake. This mechanism may account for between 60% and 80% of the rate of total glucose oxidation in awake nonstimulated human cerebral cortex, and possibly an even larger fraction of the increment in glucose oxidation with stimulation (5,90). However, there are alternate potential explanations for the *in vivo* results that need to be tested. Most importantly, it will be necessary to devise strategies for directly distinguishing glial glucose uptake from neuronal glucose uptake and phosphorylation in the intact cerebral cortex. In addition, the stoichiometry between neuronal glucose oxidation and the glutamate/glutamine cycle remains to be measured under conditions of sensory stimulation, and in different brain regions.

IN VIVO MRS STUDIES OF GABA METABOLISM AND THE EFFECTS OF DISEASE AND PHARMACOLOGIC TREATMENT ON HUMAN GABA METABOLISM

GABA is the major inhibitory neurotransmitter in the cerebral cortex (46,47). It is synthesized from glutamate in specialized cells called GABAergic neurons. The release of GABA by a GABAergic neuron inhibits the electrical activity of adjacent neurons. Extensive studies in animals and isolated brain cells and slices have shown that GABAergic function is altered in a variety of models of neurologic and psychiatric disease (46,101,102). Several antiepileptic and psychiatric drugs are targeted at the GABAergic system. GABA is overlapped in the *in vivo* ¹H MRS spectrum by the more intense resonances of macromolecules (103), glutathione, and creatine. The development of ¹H MRS spectral editing of GABA in animals and humans (6,66,104, 105) has provided a new window on studying GABA metabolism and GABAergic function in animals and humans. Several of the main findings using MRS to study alterations in GABA metabolism in disease and the effect of pharmacologic treatment on GABA metabolism are reviewed below.

MRS Studies of the Effect of the Antiepileptic Drug Vigabatrin on GABA Metabolism

Vigabatrin irreversibly inhibits the enzyme GABA transaminase (GABA-T). GABA-T catalyzes the breakdown of GABA in GABAergic neurons and in astrocytes. By inhibiting GABA-T, the drug leads to an elevation in GABA concentration. The ability of ¹H MRS editing to measure GABA elevated by GABA-T inhibitors was first demonstrated in the rat brain (106,107). Subsequent MRS editing studies of vigabatrin action on patients have made several new observations relevant to optimum administration of the drug including (a) chronic dosing above 3 g per day

patient taking vigabatrin 4 g/day**brain GABA before vigabatrin**

3.4 3.2 3.0 2.8 ppm

proton magnetic resonance spectroscopy

FIGURE 25.8. *In vivo* ^1H MRS spectra of total edited GABA from the occipital lobe of a patient with epilepsy before and after treatment with vigabatrin. The ^1H MRS spectra were obtained using spectral editing (112) from a 14-cm^3 volume centered on the midline in the visual cortex. Chronic treatment with vigabatrin led to an over twofold increase in the concentration of total edited GABA, which is the sum of GABA and homocarnosine.

fails to additionally increase GABA concentration (108), (b) GABA concentration reaches a maximum level within 2 hours of initial drug administration (109), (c) the effectiveness of vigabatrin in controlling seizures depends on elevating GABA concentration above the mean level found in nonepileptic subjects (108), (d) GABA concentration is increased by over two times the predrug concentration within 2 hours of an acute dose of 3 g of vigabatrin and remains elevated over 48 hours after a single dose of vigabatrin (109), and (5) there is no down-regulation of GABA-A receptors during chronic dosing with vigabatrin (see refs. 110 and 111 for a review of these studies). Figure 25.8 shows two edited spectra of total GABA obtained from the visual cortex before and after chronic vigabatrin treatment of a patient of epilepsy (108,112).

Cortical GABA Synthesis Is Reduced Following Prolonged GABA-Transaminase Inhibition

An initial finding in ^1H MRS studies of vigabatrin action in epilepsy patients was that the drug failed to raise GABA above a dose of 3 g/day (108). The enzymatic mechanisms controlling GABA levels *in vivo* are complex, involving short-term regulation of GAD by modulators (e.g., ATP, P_i) that affects the binding of cofactor pyridoxal phosphate, longer-term regulation involving enzyme protein levels, availability of glutamate precursors and their pathways (e.g., GABA-glutamine cycling), and postsynaptic and astroglial

catabolic pathways. GAD exists as two major isoforms (GAD_{67} and GAD_{65}) in the brain; each is the product of separate genes (113,114) and each has distinct kinetic properties (114,115). GAD_{67} is distributed throughout the cytoplasm of GABAergic neurons, whereas GAD_{65} is associated with synaptic terminals. Recently, it was shown that the 67-kd isoform of GAD protein is reduced in response to elevated levels of GABA *in vitro* and *in vivo* (116,117). Differential control of the GAD isoforms suggests that they may mediate different fluxes. To investigate the effects of elevated GABA on GABA synthesis and quantitatively assess the role of the GAD isoforms in GABA synthesis, rates of turnover of cortical glutamate and GABA were determined in anesthetized rats during an infusion of $[1\text{-}^{13}\text{C}]$ glucose after administration of the GABA-transaminase inhibitor vigabatrin (500 mg/kg, i.p.), to increase GABA levels (24). GABA concentration was increased twofold at 24 hours. Tricarboxylic acid cycle flux was not affected by vigabatrin treatment compared to nontreated rats despite the increased GABA level. An analysis of the turnover data revealed a $\sim 70\%$ decrease in the rate of GABA synthesis following vigabatrin-treatment (control, $0.14 \mu\text{mol/g/min}$; vigabatrin-treated, $0.04 \mu\text{mol/g/min}$). The reduction in GABA synthesis concomitant with the selective inhibition of GAD_{67} suggests that GAD_{67} accounts for the major fraction of GABA synthesis in the rat cerebral cortex under anesthetized nonstimulated conditions. This conclusion is supported by studies of GAD_{67} and GAD_{65} in knockout mice (118,119), which have found an order of magnitude greater reduction in GABA concentration in the mice with a GAD_{67} knockout. The isoform composition of human brain is presently unknown.

Elevation of GABA by Other Antiepileptic Drugs

^1H MRS studies have found that several antiepileptic drugs, with no known metabolic mechanisms of action on the GABAergic system, also lead to a rapid elevation of GABA concentration. These drugs include GABA-pentin, topiramate, and lamotrigine (120–124). The elevation of GABA may be an important mechanism in the effectiveness of these medications as antiepileptic compounds. In addition, these findings provide evidence that the regulation of GABA metabolism is tightly integrated with the regulation of GABAergic function. Figure 25.9 shows a time course of the elevation of GABA after administration of an acute dosage of topiramate. As with vigabatrin, the concentration of GABA reaches a maximum of two times the predrug concentration within 2 hours of drug administration. A similar rapid elevation of GABA was measured after an acute dosage of GABA-pentin (122,124). The ability of ^1H MRS to track the response of the GABAergic system to pharmacologic therapy may potentially be useful for developing optimum dosing strategies.

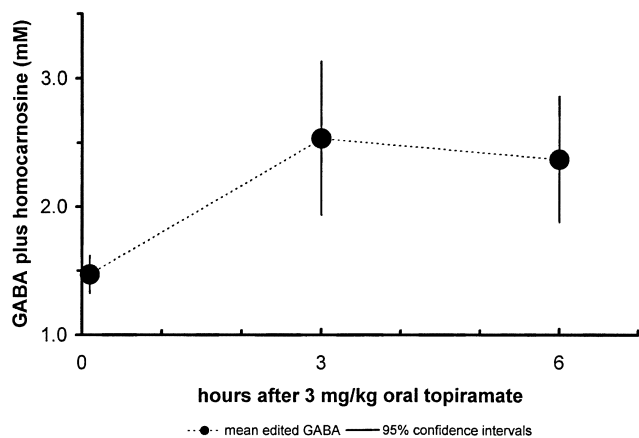


FIGURE 25.9. A time course of GABA plus homocarnosine concentration after administration of topiramate. Topiramate at 3 mg/kg was administered to six volunteers without epilepsy. ^1H MRS spectral editing measurements were performed at 4 T (123). GABA levels were measured to peak within 3 hours after administration of topiramate at approximately two times the predrug levels. A study looking at the acute effect of topiramate on GABA levels of epileptic patients found that the increase was almost entirely due to GABA (121). The GABA plus homocarnosine concentrations are normalized to a creatine concentration of $9\ \mu\text{mol/g}$ for comparison with measurements by Petroff and co-workers (111), and the predrug concentrations are in excellent agreement. (Redrawn from Kuzniecky RI, Hetherington HP, Ho S, et al. Topiramate increases cerebral GABA in healthy humans. *Neurology* 1998;51:627–629.)

Effects of Neurologic and Psychiatric Disease on GABA Concentration

Impaired GABAergic function has been implicated in the etiology of epilepsy (101). Consistent with this proposal, ^1H MRS editing studies have found decreased GABA in adult epilepsy (111,125) and pediatric epilepsy (126). In epilepsy the release of cytosolic GABA has been proposed as an important mechanism for seizure suppression (127, 128). The finding that a low GABA concentration was strongly associated with poor seizure control in epilepsy supports this proposal. Further support for a role of cytosolic GABA concentration in inhibiting cortical excitability comes from the finding that the improvement in seizure control of subjects administered vigabatrin chronically depended on the elevation of cerebral cortex GABA concentration (108).

In addition to epilepsy, reduced GABA concentration has been found in unipolar depression (129), alcohol withdrawal, and hepatic encephalopathy (130). These disorders are associated with an alteration in inhibitory GABAergic function. The finding of low GABA associated with these disorders is additional evidence that the brain metabolic GABA pool has an important role in GABAergic function. The finding in unipolar depression appears paradoxical because the condition is not associated with enhanced cortical excitability. A potential explanation of this finding is that

the low GABA concentration in this disease is a compensation for the reduction in excitatory glutamatergic activity (129).

Parsing the Edited GABA Resonance

The edited GABA resonance consists of GABA and the GABA derivative homocarnosine, which is a condensation product of GABA and histidine. Homocarnosine is a neuro-modulator present in a specific subclass of GABAergic neurons in the primate brain. Short TE ^1H MRS with macromolecule suppression may be used to measure the homocarnosine histidine proton resonances in the downfield region of the short TE spectrum (103,112). Combining the homocarnosine measurement and the total GABA editing measurements has allowed the separate measurement of homocarnosine and GABA. Through modification of the editing selectivity, the GABA derivative pyrrolidinone may also be measured in the edited spectrum (131). It was recently shown that GABA, homocarnosine, and pyrrolidinone have different time courses in response to a first-time challenge with vigabatrin (109).

Estimate of the GABA/Glutamine Cycle in Nonstimulated Human Cerebral Cortex

The *in vivo* ^{13}C MRS measurement may potentially be extended to study the rate of GABA synthesis and the GABA/glutamine cycle (34,65). However, the ability to directly measure GABA synthesis at 2.1 T is limited by the $[2-^{13}\text{C}]$ GABA resonance being overlapped at 2.1 T by the isotopomer sideband of the $[4,3-^{13}\text{C}]$ glutamate resonance. Due to the entry of GABA into the glial TCA cycle at the level of succinate, the labeling kinetics of C4-glutamine derived from GABA are indistinguishable from label entering through anaplerosis. From the results of Shen et al. (29), the maximum estimate of the rate of the GABA/glutamine cycle, obtained by assuming that V_{ana} is entirely due to GABA, would be approximately 10% of the rate of glutamine synthesis (29). In the 4-T studies of Gruetter et al. (13,35), the C2 resonance of GABA was resolved (Fig. 25.2), which indicates that direct quantitation of the rate of GABA synthesis and the GABA/glutamine cycle will be possible in human cerebral cortex at higher field strengths.

Summary and Remaining Questions

The ability of ^1H MRS to measure regional levels of GABA and GABA derivatives has provided a new window on the GABAergic system in neurologic and psychiatric disease. Reduced levels of cerebral cortex GABA have been found in patients with adult and pediatric epilepsy, depression, and alcohol withdrawal. Studies have found that several of the new generation of antiepileptic drugs raise GABA levels,

and GABA elevation may be related to their effectiveness in seizure depression. The recently demonstrated ability to perform GABA spectroscopic imaging (105) opens up the potential for using regional variations in GABA level diagnostically and to track the effectiveness of drugs targeted at the GABAergic system.

Two important questions are raised by these findings: What is the relationship between GABA levels and the rate of the GABA/glutamine cycle? What is the relationship between the GABA/glutamine cycle and cortical excitability? A preliminary study has recently demonstrated the ability to use isotopic labeling strategies, similar to those developed to measure the glutamate/glutamine cycle, to measure the rate of the GABA/glutamate cycle (39). This strategy, in combination with the manipulation of GABA levels either pharmacologically or through transgenic methods, may provide significant insight into how the regulation of GABA concentration affects GABAergic function.

IN VIVO MRS MEASUREMENTS OF NEUROENERGETICS DURING FUNCTIONAL ACTIVATION

Under physiologic conditions brain oxygen and glucose consumption are tightly coupled (49), with between 90% and 95% of glucose uptake being completely oxidized. The tightness of this coupling during brain activation was questioned when Fox and co-workers (132) measured by PET a mean increase of 51% in CMR_{glc} in the primary visual cortex of humans during stimulation by a flashing checkerboard pattern accompanied by only a 5% increase in oxygen consumption ($CMRO_2$). This finding was surprising because of the 16- to 18-fold lower ATP production from nonoxidative glycolysis compared with the complete oxidative consumption of glucose. It was concluded from these results that the energy for supporting electrical activity derives primarily from nonoxidative glycolysis as opposed to glucose oxidation (132,133). More recently, the greater increase in cerebral blood flow than oxygen consumption that leads to the BOLD (blood oxygenation level dependent) effect has been taken as evidence of the hypothesis of stimulated neuronal activity requiring little energy (134).

The apparently minimal need for energy from glucose oxidation to support stimulated neuronal activity is paradoxical because of the considerable evidence that the majority of energy consumption in the nonstimulated brain, which primarily uses glucose oxidation, is to support neuronal electrical activity. This evidence includes the critical dependence of brain function on oxygen delivery, the 50% to 70% reduction of brain energy requirements under isoelectric conditions (133), and the ^{13}C MRS findings of a high activity of the glutamate/glutamine cycle in the resting awake brain and the linear coupling of this rate to neuronal glucose oxidation (see the above sections In Vivo MRS Mea-

surements of the Rate of the Glutamate/Glutamine Cycle: Findings and Validation, and Determination of the *In Vivo* Coupling Between the Rate of the Glutamate/Glutamine Neurotransmitter Cycle and Neuronal Glucose Oxidation). Furthermore, there is no cellular evidence that stimulated and nonstimulated neuronal activity have different energetic requirements. As discussed below (see Implications of MRS Studies for Understanding Brain Function), the ambiguity created by the variable degree of uncoupling between glucose consumption and oxidation hinders the interpretation of the functional imaging signal quantitatively in terms of changes in neuronal activity.

MRS provides a powerful tool for studying the question of metabolic coupling between glucose and oxygen by allowing measurements of the rates of nonoxidative glycolysis and glucose oxidation. MRS experiments have shown that under stimulated conditions the majority of energy for functional activity is from glucose oxidation (14,15,135). They have also confirmed the presence of metabolic uncoupling at high levels of brain activity (136–138). A model has been proposed to explain the uncoupling of glucose consumption and oxidation during certain types of stimulation as an extension of the normal energetic processes used to support the glutamate/glutamine cycle (139).

MRS Studies of Lactate Generation and Glucose Oxidation During Sensory Stimulation

A prediction of the presence of uncoupling of the increase of glucose consumption and oxidation during visual activation is that there will be an elevation of lactate in the visual cortex. Several laboratories have found an increase in lactate concentration (136–138) during visual stimulation of the human visual cortex by 1H MRS of approximately 0.2 to 4 $\mu\text{mol/g-min}$ within 2 to 6 minutes of activation. The small increase in lactate is consistent with earlier findings in animal models (40).

The degree of mismatch between the increase in glucose consumption and oxidation during sensory stimulation was studied by Hyder and co-workers (14,15) using forepaw stimulation of an anesthetized rat measured the rate of increase in neuronal glucose oxidation from the ^{13}C isotopic turnover of glutamate using POCE (proton observe carbon edit) heteronuclear editing. These studies found a large increase in the rate of glucose oxidation during sensory stimulation (Fig. 25.10). This increase was in good agreement with previous measurements of the increase in total glucose consumption (140). While within the accuracy of the measurements there was room for a significant rate of nonoxidative glycolysis, the contribution of nonoxidative glycolysis to total cerebral ATP production during activation would be minor due to the much greater number of ATP molecules produced by the complete oxidation of glucose (32–36) than by nonoxidative glycolysis to lactate (2).

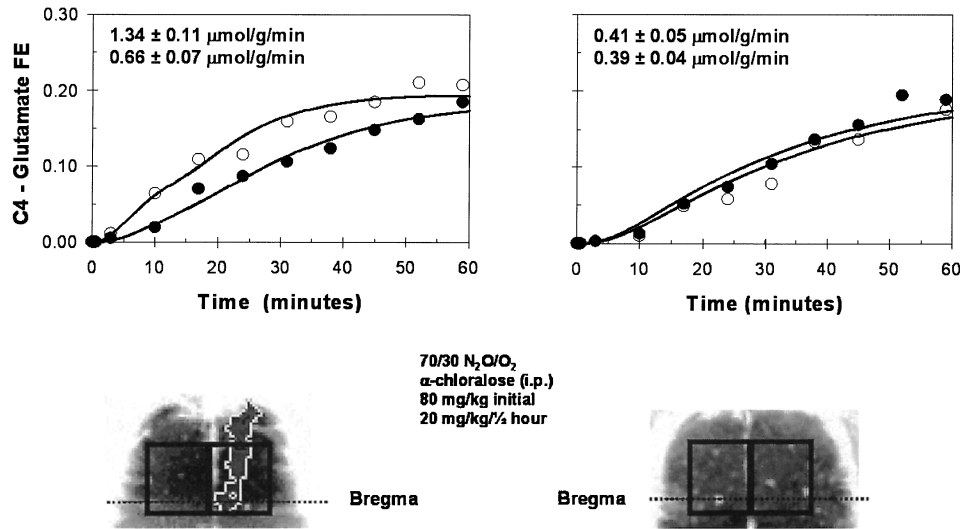


FIGURE 25.10. Time course of C4 glutamate labeling in the ipsi- and contralateral somatosensory cortex of a rat during single forepaw electrical stimulation. *In vivo* ^1H - ^{13}C MRS spectra were obtained from two 24- μL volumes, positioned in the ipsi- and contralateral somatosensory cortex of rats at 7 T. The spectroscopic volumes are superimposed on a coronal image. The time courses on the right shows the labeling of C4-glutamate during the infusion of a control rat. The time courses on the left were obtained during single forepaw electrical stimulation. The *lighter region* on the image obtained during stimulation is the superposition of the blood oxygenation level dependent (BOLD) functional MRI (fMRI) obtained during the study. The rate of labeling on the contralateral side to the stimulation is observed to increase to approximately two times the rate of the ipsilateral side. The rates on the figure are the calculated rates of the TCA cycle from the group of rats studied in the contra- and ipsilateral volumes. (Redrawn with data from Hyder F, Rothman DL, Mason GF, et al. Oxidative glucose metabolism in rat brain during single forepaw stimulation: a spatially localized ^1H [^{13}C] NMR study. *J Cereb Blood Flow Metab* 1999;17: 1040–1047.)

Calculation of the Relative Contributions of Glucose Oxidation and Nonoxidative Glycolysis to the Incremental Energy Production During Brain Activation

Two recent papers reviewed the increase in glucose oxidation during cognitive and sensory reported in a large number of studies, and concluded that in almost all reports the majority of incremental energy production is from glucose oxidation (131,141). Table 25.1 presents the measured fractional change in the rate of total glucose consumption (cerebral metabolic rate of glucose metabolism, CMR_{glc}) and oxidation (cerebral metabolic rate of oxygen, CMRO_2) in the human visual cortex during visual stimulation. The studies tabulated used either PET or quantitative functional MRI (fMRI) (142–149). In most cases the increase in CMRO_2 is greater than reported by Fox et al. (132), and the increase in CMR_{glc} is less. These differences have been attributed to differences in stimulation paradigms, with greater uncoupling from simple stimuli and almost complete coupling from complex stimuli (142,149). As shown in the table, even in the most extreme reports of uncoupling the fraction of the increment in total ATP production supplied by glucose oxidation is larger than that supplied by nonoxidative glycolysis.

A limitation of both the PET and quantitative fMRI measurements of oxygen consumption is that they depend on assumptions about blood flow/oxygen delivery coupling in order to derive rates (131). The measurement of glucose oxidation by MRS gets around the requirement of detailed knowledge, or calibration, of this parameter by directly measuring the flow of labeled glucose into the TCA cycle. The recent demonstration of high spatial resolution POCE measurements of glucose oxidation in human visual cortex at 4 T indicate that this method is ready to address this question in the human visual and other sensory systems (31,44).

The Glycogen Shunt, a Model of the Mismatch Between Glucose Consumption and Oxidation During Stimulated Neuronal Activity

The results tabulated in Table 25.1 show that the degree of mismatch between the increment in glucose consumption and glucose oxidation is the greatest for stroboscopic stimuli, which require alternate periods of intense activation followed by a quiescent period. For example, in visual stimulation the greatest mismatch was reported for a flashing red dot matrix (132), while no mismatch was found for

TABLE 25.1. NEUROENERGETIC YIELD WITH STIMULATION

Stimulation	$\Delta\text{CMR}_{\text{glc}}$ (%)	$\Delta\text{CMR}_{\text{O}_2}$ (%)	Energy Yield (%)		Reference
			(non-ox) CMR_{glc}	(ox) CMR_{glc}	
Visual	51	5	38	62	Fox et al. (132)
	28	28	6	94	Marrett and Gjedde (142)
	29	29	7	93	Marrett and Gjedde (142)
	(31)	16	(10)	90	Davis et al. (143)
	23	(20)	6	(94)	Chen et al.
	24	(20)	6	(94)	Reivich et al. (144)
	(31)	25	(7)	93	Hoge et al. (145)
	(31)	30	(6)	94	Kim et al. (146)
	(31)	5	(27)	73	Kim and Ugurbil (147)
	Average	31	20	8	92
Seizure	400	267	8	92	Borgstrom et al.

Tabulated are the reported increments in CMR_{glc} and CMR_{O_2} from studies using positron emission tomography (PET) or quantitative functional magnetic resonance imaging (MRI) to measure these parameters. The increase in adenosine triphosphate (ATP) production was calculated for each study using a value of 2 ATP molecules produced per glucose molecule consumed in the glycolytic pathway, and 32 additional ATP molecules produced when glucose is completely oxidized. The energy yield is expressed as the percent of the total increase in ATP production from nonoxidative glycolysis [(non-ox) CMR_{glc}] and the oxidative breakdown of glucose in the TCA cycle [(ox) CMR_{glc}]. As shown in the table, even in the most extreme reported cases of uncoupling between CMR_{glc} and CMR_{O_2} the majority of ATP production is from glucose oxidation due to the greater ATP yield. CMR, cerebral metabolic rate.

the increase from a colored alternating radial checkerboard, which produces a continuous level of stimulation (142,149). The largest sustained mismatch between glucose consumption and oxidation occurs in bicuculline-induced status epilepticus where total glucose consumption increases to fourfold the prestatus value, whereas oxidation is increased twofold (49,148). In bicuculline-induced status epilepticus, brain cerebral cortex electrical activity is characterized by a burst of intense firing followed by a suppressed period of little electrical activity.

We have proposed a model to explain these observations based on the requirement for ATP from glial glycolysis to supply the ATP needed for glial glutamate clearance and glutamine synthesis (see Determination of the *In Vivo* Coupling Between the Rate of the Glutamate/Glutamine Neurotransmitter Cycle and Neuronal Glucose Oxidation, above). In this model the majority of glucose required to fuel the pumping of glutamate from the synaptic cleft during the intense bursts of neuronal firing induced by sensory stimulation is provided by brain glycogen (150,151). Glycogen phosphorylase is kinetically well suited for rapid increases in activity through its regulation by signaling pathways and phosphorylation. There is *in vivo* evidence that brain glycogen may be rapidly mobilized to support function including in status epilepticus (49) and in physiologic brain activation (152–154). In the glycogen shunt model, after an initial period of glycogen depletion during intense stimulation, a steady state is reached in which the glycogen used to rapidly generate ATP for the transport of glutamate into the glial cell and conversion to glutamate during bursts of intense activity is resynthesized during the interim quiescent periods. Only one ATP molecule is produced per glu-

cose moiety used by this pathway, instead of the two produced by glycolysis, and therefore the stoichiometry between the glutamate/glutamine cycle and glial glucose uptake changes to 1:1 from 1:2. The 1:2 ratio is approximately the ratio measured during status epilepticus, in which almost all cortical electrical activity is involved in a burst and suppress pattern. The presence of simultaneous synthesis and breakdown of glycogen has been demonstrated in the exercising muscle (155), and more recently in the cerebral cortex of the stimulated and anesthetized rat (152). Figure 25.11 describes the model schematically.

Summary and Remaining Questions

In vivo MRS studies have made significant contributions to the understanding of functional neuroenergetics. The measurement of the glutamate/glutamine cycle under different levels of electrical activity (see the above sections *In Vivo* MRS Measurements of the Rate of the Glutamate/Glutamine Cycle: Findings and Validation, and Determination of the *In Vivo* Coupling Between the Rate of the Glutamate/Glutamine Neurotransmitter Cycle and Neuronal Glucose Oxidation) has shown that the majority of brain energy production in even the nonstimulated state supports neuronal activity. Several MRS studies have provided insight into the mismatch between glucose consumption and oxidation during sensory stimulation. Lactate elevation during visual stimulation provided direct validation of the findings using PET (132) of the mismatch between oxygen consumption and glucose consumption (136–138). Although there is a significantly greater increase in glucose consumption than oxidation in certain stimulated states, studies of

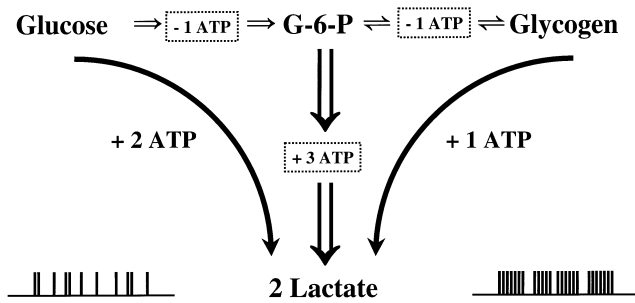


FIGURE 25.11. A schematic diagram of the glycogen shunt model. Glucose taken up by the glia can flow through two pathways after phosphorylation to glucose 6-phosphate. In the standard pathway (*left arrow*), which occurs during normal electrical activity, glucose 6-phosphate is directly converted to lactate by glycolysis producing two ATP molecules per glucose molecule. The stoichiometry between glucose uptake and glutamate transport is 1:1 in this pathway. The majority of lactate is subsequently oxidized in the neuron. In the glycogen shunt pathway (*right arrow*), which occurs during intense repeated bursts of electrical activity, such as in seizures or intense sensory stimulation, glucose is synthesized into glycogen first before being converted to lactate. An ATP molecule is used in the synthesis of glycogen, resulting in a reduction in the energetic yield from the pathway to one ATP molecule per glucose molecule. The stoichiometry between glucose uptake and glutamate transport is increased to 2:1 in this pathway. The extra lactate produced in the shunt pathway is not required for neuronal energy metabolism and eventually leaves the brain.

the rate of neuronal glucose oxidation during sensory stimulation in the rat cerebral cortex have shown that neuronal glucose oxidation provides the majority of energy production in the stimulated state (14,15). The conclusion derived from the MRS studies is consistent with PET measurements of the mismatch when the much greater efficiency of ATP production from glucose oxidation is taken into account (135), as shown in Table 25.1. A potential explanation of the mismatch has been proposed based on the requirement for rapid glycolytic energy generation to clear glutamate from the synaptic cleft during the bursts of intense neuronal firing associated with stimulated neuronal activity (151). In this glycogen shunt model, the power required is provided by rapid glycogen breakdown. The glycogen is resynthesized during the inter-burst periods resulting in a reduction in the normal stoichiometry between glutamate transport into the glia and glial glucose uptake from 1:1 to 1:2.

Several major questions remain to be addressed on the neuroenergetic support of functional activity. Paramount among these is the need for a measurement of the glutamate/glutamine cycle during sensory stimulation. In addition, although the majority of the increase in energy consumption during stimulation is associated with glutamatergic neurons (15,156), the relative contributions of glia and GABAergic neurons are not known. At present there are only minimal data from brain studies supporting the glycogen shunt model of the mismatch between glucose consumption and oxidation. Studies measuring glycogen turnover directly

under these conditions (30) may be able to directly test this hypothesis, and better establish the role of glycogen in functional neuroenergetics.

IMPLICATIONS OF MRS STUDIES FOR UNDERSTANDING BRAIN FUNCTION

The stoichiometry of the rate of the glutamate/glutamine cycle and oxidative glucose metabolism has implications for connecting models of brain function at the macroscopic level, as studied by functional imaging, with neurobiological studies at the level of synapses and networks of neurons. This section reviews work in which this relationship was used to calibrate the PET and fMRI signals and neuroenergetic signals, which are either indirectly or directly measures of functional glucose metabolism, with neurotransmitter cycling (5,139,157). Some implications of this calibration for the interpretation of brain functional imaging are explored.

Calibration of the Relationship Between the Glutamate/Glutamine Cycle and the PET and BOLD MRI Functional Imaging Signal

At present, functional PET and fMRI are not quantitated in terms of specific neuronal processes involved in information transfer. The functional imaging signal in PET and fMRI is either directly or indirectly coupled to the change in glucose oxidation with activation (1,2,134). The tight coupling between the glutamate/glutamine cycle and neuronal glucose oxidation in the rat cerebral cortex (26,90) provides a relationship for calibrating the functional imaging signal to the specific neuronal process of glutamate release and recycling (5).

The similarity of the ratio of the rates of the glutamate/glutamine cycle to neuronal glucose oxidation in human cerebral cortex and the rat cerebral cortex supports a similar relationship holding for the awake nonstimulated human cerebral cortex. Although studies are needed to establish the exact stoichiometry during sensory or other external stimulation, it is reasonable to extrapolate a positive (and possibly stoichiometric) relationship between changes in the rate of neuronal glucose oxidation and the glutamate/glutamine cycle during activation. Using this relationship, the functional imaging signal may be converted to a first order to changes in the rate of glutamate/glutamine neurotransmitter cycle (5). The advantage of performing this calibration over the direct MRS measurement of the glutamate/glutamine cycle is that several orders of magnitude of higher spatial and temporal resolution is possible with the MRI measurement.

Estimate of the Total Neuroenergetics Used to Support Functional Neuronal Activity During Sensory Stimulation

An assumption in the conventional interpretation of functional imaging is that the increment in neuronal activity during brain activation is sufficient to support the incremental mental processes in a region during sensory stimulation or a cognitive task (5). This interpretation is trivially valid if there is insignificant neuronal activity in the non-stimulated state. The high rate of the glutamate/glutamine neurotransmitter cycle found by ^{13}C MRS in the nonstimulated brain raises the question of whether the incremental neuronal activity is sufficient for mental processing or if the total regional neuronal activity is needed. This question was addressed by analyzing previous studies that measured the change in glucose consumption during stimulation in the sensory cortices of animals stimulated under anesthetized and awake conditions. The studies chosen used anesthetics that interfere minimally with the electrical response to sensory stimulation (157). During anesthesia, the baseline glucose consumption was reduced by as much as two- to three-fold. Based on the standard paradigm, a constant increment of neuronal activity, and by inference glucose consumption, during stimulation would be expected regardless of whether the animal was anesthetized or awake. In contrast, if the majority of regional neuronal activity was required for sensory processing, then the glucose consumption required during stimulation would be similar whether the animal was awake or anesthetized. The prediction of these two models is diagrammed in Fig. 25.12. Results from a number of studies indicated that a similar level of cortical activity was reached during stimulation, independent of the degree of suppression of resting glucose consumption by the anesthesia (139, 157). These results were supported by the MRS studies that found a large increment in glucose oxidation with somatosensory stimulation under α -chloralose anesthesia (15,156). This finding supports the view that during stimulation the total neuronal activity in sensory regions is required to support brain function. Results of this literature survey have recently been reinforced by similar results using quantitative MRI to measure changes in oxygen consumption in the same animal at two different levels of anesthesia (158).

Implications of the Calibration of the Functional Imaging Signal on the Standard Interpretations of Functional Imaging Studies

The goal of many functional imaging studies is to determine the anatomic location of brain regions involved in performing mental processes. To achieve this goal, subjects are given cognitive or motor tasks to perform, or exposed to sensory stimulation, while being scanned. The degree of involvement of a region in the performance of a task is determined

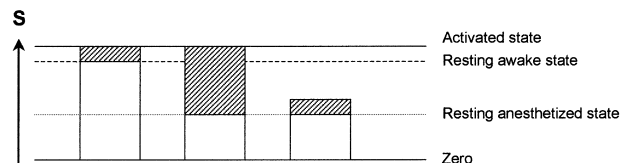


FIGURE 25.12. Schematic representation of possible increase in the functional imaging signal, as measured by neuroenergetics, upon sensory stimulation for an animal that is nonanesthetized (A) and anesthetized (B,C). The difference in the magnitude of the functional imaging signal, as quantified by glucose oxidation, between stimulated and nonstimulated states is represented by the shaded rectangles. In functional imaging these increments are commonly used to identify focally activated regions. The remaining signal, which is represented by white rectangles, is removed by fMRI analysis methods. ^{13}C MRS studies have shown that a large fraction of the total signal is from neuroenergetic processes coupled to neuronal activity. If the neuronal activity needed to perform the task was the same as the increment from the awake state, then the increase in the signal upon stimulation would be the same for the anesthetized or awake states (compare A and C). If instead a large fraction of the total neuronal activity in the region supports the sensory processing, then the incremental signal from anesthesia would be much larger (compare A and B). A survey of results in the literature showed that in most cases, when anesthetics such as α -chloralose that do not block stimulated electrical activity are used, the total glucose consumption and oxidation rises to the same absolute level during stimulation independent of the initial awake state. These results support the magnitude of the neuronal activity required to support a task (B) being substantially larger than the increment in neuronal activity over the resting awake state (C). (From Shulman RG, Rothman DL, Hyder F. Stimulated changes in localized cerebral energy consumption under anesthesia. *Proc Natl Acad Sci USA* 1999;96:3245–3250, with permission.)

by the increment in the magnitude of the imaging signal relative to the signal when the subject is in a resting state, or performing some other task. An implicit assumption in this analysis often used is that the size of the increment of the signal is proportional to the total neuronal activity recruited by these mental processes (3,5,159).

As described above, MRS studies have shown that the total neuronal activity in a region, as quantified by the glutamate/glutamine cycle, is much larger than the incremental increase with functional activation. The impact on interpretation of knowing the total magnitude of, as opposed to the incremental, neuronal activity associated with the processing of a stimulus or task may be illustrated through a simple example. Consider a hypothetical experiment in which two subjects perform a cognitive task. In one subject the regional increment in the functional imaging signal in the frontal lobe, quantified as the change in the rate of glucose oxidation, is 1% of the resting rate of total glucose oxidation. In the second subject the same task induces a signal/rate increment of 2%. In the standard interpretation, the second subject recruited twice the neuronal activity to perform the task as the first subject. If instead these increments are calibrated as increments in the glutamate/glutamine cycle the relative difference in neuronal activity is only

a few percent. This example shows that knowing the total size of the signal associated with neuronal activity is important in cases where inferences are being made about differences in the level of neuronal activity, such as when functional imaging is used to study the effects of drugs or disease on brain function (139,160). It is also important in the interpretation of functional imaging data to locate a mental process or function (5).

Implications for Studies of Brain Function

The prevailing theory used to interpret functional imaging studies, particularly of cognitive processes, is based on cognitive psychology (3,139,159,161). In the cognitive psychology model of the brain, complex mental processes are broken down using information theory into component processes, sometimes called modules. Functional imaging is used to locate these postulated modules. The search for specialized functional areas has been facilitated by analysis methods such as statistical parametric mapping. These methods identify regional changes in the imaging signal based on the statistical significance of the temporal correlation of the signal changes with the mental processes postulated by the investigator (which are expressed in the design matrix) involved in performing a task (162). In the statistical representation of brain activity, the magnitude of the regional neuronal activity is often ignored in favor of a binary representation as “active” and “inactive.” Statistical methods have been widely adopted to analyze fMRI data. A key assumption often used in the statistical representation of brain function is that the regional neuronal activity used for performing a mental process is independent and separable from the activity of other regions (162,163), as well as the neuronal activity recruited by other processes being supported within the same region.

The use of MRS to calibrate neuroimaging provides the potential for examining complex regional brain interactions that do not fulfill the strict modular criteria of independence. Several lines of experiments have shown that parallel regional brain functions interact, and alter the magnitude of the neuronal activity used in processing a stimulus or task (163–165). An example are the studies by Desimone’s group (164) on the effect of attention upon the neuronal activity, as measured by the distribution of single neuron firing rates in a region, associated with visual perception. An illustrative set of experiments used two closely spaced visual signals within the same receptor field of a particular region of the striate cortex. The change in neuronal firing rate obtained from one stimulus was found to depend critically on the degree of attention paid to the nearby stimulus. Consistent with this result, an effect of attention on the magnitude fMRI BOLD signal in the human extrastriate cortex has been reported (165,166). The calibration of the functional imaging signal in terms of the glutamate/gluta-

mine cycle will extend these studies by allowing these interactions between regions to be described quantitatively in terms of neuronal activity changes, as is presently done only in electrophysiology studies of animal cerebral cortex. This quantitation should allow the exploration of these complex interactions in much finer detail in humans than is presently possible.

In addition to providing enhanced capability to understand horizontal interactions between brain regions, the calibration of neuroimaging by MRS also allows a vertical dimension of neuronal activity to be explored. The MRS finding of a high rate of the glutamate/glutamine cycle even under nonstimulated conditions is consistent with recent experimentally based proposals that maintaining a constant high level of neuronal activity is critical for brain function. Two recent experiments support this hypothesis. The need for substantial unfocused neuronal activity for the service of even sensory responses was suggested by a recent experiment of Grinvald’s group (167). Starting with the recognition that “cortical neurons are spontaneously active in the absence of external input even in primary sensory areas,” the authors studied the correlation between single-unit recordings and real-time optical imaging, which provided a measure of total neuronal activity in the region. They concluded by suggesting that “in the absence of stimulation the cortical network wanders through various states represented by coherent firing of different neuronal assemblies,” and that a stimulus pushes the network into a state representing the stimulus. Analogously, Singer (168) measured the temporal synchronization of neuronal responses and concluded, “Of the many responses of V1 those that become synchronized best will be particularly effective in influencing neurons in higher areas.” These studies both support the presence of a large amount of neuronal activity in the unstimulated state and suggest a role for this activity in brain function. The results from MRS studies provide quantitative measures of the total amount of stimulated and unstimulated activity in a region, and thereby can provide a quantitative basis for analysis.

SUMMARY AND CONCLUSIONS

Below is a summary of the major findings of MRS studies of the glutamate/glutamine cycle, GABA/glutamine cycle, and functional neuroenergetics, and some of the implications of these findings for understanding brain function.

Approximately 60% to 80% of total glucose oxidation (and energy consumption) in the nonstimulated cerebral cortex is by glutamatergic neurons, with most of the remainder in GABAergic neurons and glia (13,18,24,26,27,29,35,38).

The energetic needs of glutamatergic and GABAergic neurons and glia dominate cerebral cortex energy requirements.

In the awake nonstimulated cerebral cortex of humans

and rats, the rate of the glutamate/glutamine cycle is 60% to 80% of total glucose oxidation (13,26,29,35):

1. Glutamate release and recycling is a major metabolic pathway.
2. Glutamate metabolism and neurotransmission can no longer be conceptually separated.
3. The nonstimulated awake brain has a high level of neuronal activity, most likely greater than the increment in activity with external stimulation.

The rate of the glutamate/glutamine cycle increases linearly with neuronal glucose oxidation in a close to 1:1 stoichiometry (26):

1. Energy metabolism in cortical glutamatergic neurons is tightly coupled to glutamate release and recycling.
2. The stoichiometry supports a model in which astrocyte glucose uptake is coupled mechanistically to the glutamate/glutamine cycle (90) through the need for glycolytic ATP to transport glutamate into the astrocyte and synthesize glutamine.
3. The increase in glucose consumption measured during functional activation may be directly coupled to the glutamate/glutamine cycle, providing a calibration for the functional imaging signal.

The GABA level in human cerebral cortex is reduced in epilepsy, alcohol withdrawal, and depression and is raised by several pharmacologic treatments (111,129):

1. The concentration of the metabolic pool of brain GABA may play a critical role in inhibitory GABAergic function.
2. Measuring cerebral cortex GABA level provides a useful index of brain GABAergic function and the effectiveness of certain antiepileptic drugs.

Reduction in the activity of GAD₆₇ by elevation of GABA leads to a major reduction in the rate of GABA synthesis under nonstimulated conditions (24):

1. GAD₆₇ is the major enzyme controlling nonstimulated GABA synthesis in the rat cerebral cortex.
2. Through regulation of GABA concentration GAD₆₇ may play a key role in the etiology and pharmacology of epilepsy and other neurologic and psychiatric disorders.
3. The ability of ¹³C MRS to measure the rate of GABA synthesis in combination with GABA/glutamine neurotransmitter cycling (39) may allow the functional roles of GAD₆₅ and GAD₆₇ isoforms to be distinguished quantitatively.

The glycogen shunt model provides a mechanistic explanation for the apparent uncoupling of glucose consumption and oxidation during sensory stimulation (151).

The majority of energy to support incremental and total neuronal activity during sensory stimulation is provided by neuronal oxidative glucose metabolism (14,131,156):

1. The total as opposed to incremental neuronal activity is required to support brain function during sensory stimulation (143).
2. A large amount of unfocused neuronal activity in the nonstimulated state is required for brain function.

ACKNOWLEDGMENTS

We gratefully acknowledge grant support from the National Institute of Health—DK-27121 (R.G.S.), NS-32126 (D.L.R.), HD-32573 (K.L.B.), NS-34813 (K.L.B.), NS-37203 (F.H.), RO1-NS032518, PO1-NS06208 (O.A.C.-P.)—and the National Science Foundation—DBI-9730892 (F.H.). We benefited greatly from discussions with Dr. James Lai on the localization and kinetics of key enzymes in glycolysis and the glutamate/glutamine cycle and the careful reading of the manuscript by Dr. Vincent Lebon.

REFERENCES

1. Sokoloff L. Relationship between functional activity and energy metabolism in the nervous system: whether, where and why? In: Lassen NA, Ingvar DH, Raichle ME, et al., eds. *Brain work and mental activity*. Copenhagen: Munksgaard, 1991:52–64.
2. Fitzpatrick SM, Rothman DL. New approaches to functional neuroenergetics. *J Cognit Neurol* 1999;11:4:467–471.
3. Raichle ME. Behind the scenes of functional brain imaging: a historical and physiological perspective. *Proc Natl Acad Sci USA* 1998;95:576–772.
4. Shephard GM. *The synaptic organization of the brain*. Oxford: Oxford University Press, 1994.
5. Shulman RG, Rothman DL. Interpreting functional imaging studies in terms of neurotransmitter cycling. *Proc Natl Acad Sci USA* 1998;95:11993–11998.
6. Rothman DL, Behar KL, Hetherington HP, et al. Homonuclear 1H-double resonance difference spectroscopy of the rat brain in vivo. *Proc Natl Acad Sci USA* 1984;81:6330–6334.
7. Rothman DL, Novotny EJ, Shulman GI, et al. ¹H-[¹³C] NMR measurements of [4-¹³C]-glutamate turnover in human brain. *Proc Natl Acad Sci USA* 1992;89:9603–9606.
8. Behar KL, Petroff OAC, Prichard JW, et al. (1986) Detection of metabolites in rabbit brain by ¹³C NMR spectroscopy following administration of [1-¹³C]glucose. *Magn Reson Med* 1986;3: 911–920.
9. Fitzpatrick SM, Hetherington HP, Behar KL, et al. The flux from glucose to glutamate in the rat brain in vivo as determined by ¹H-observed, ¹³C-edited NMR spectroscopy. *J Cereb Blood Flow Metab* 1990;10:170–179.
10. Cerdan S, Künnecke B, Seelig J. Cerebral metabolism of [1,2-¹³C₂] acetate as detected by in vivo and in vitro ¹³C NMR. *J Biol Chem* 1990;265:12916–12926.
11. Gruetter R, Novotny EJ, Bouleware SD, et al. Direct measurement of brain glucose concentrations in humans by ¹³C NMR spectroscopy. *Proc Natl Acad Sci USA* 1992;89:1109–1112.
12. Gruetter R, Novotny EJ, Bouleware SD, et al. Localized ¹³C. Neurochem NMR spectroscopy in the human brain of amino acid labeling from ¹³C glucose. *J Neurochem* 1994;63: 1377–1385.

13. Gruetter R, Seaquist ER, Kim S, et al. Localized in vivo ^{13}C -NMR of glutamate metabolism in the human brain: initial results at 4 Tesla. *Dev Neurosci* 1998;20:380–388.
14. Hyder F, Chase JR, Behar KL, et al. Increased tri-carboxylic acid cycle flux in rat brain during forepaw stimulation detected with ^1H - ^{13}C NMR. *Proc Natl Acad Sci USA* 1996;93:7612–7617.
15. Hyder F, Rothman DL, Mason GF, et al. Oxidative glucose metabolism in rat brain during single forepaw stimulation: a spatially localized ^1H - ^{13}C NMR Study *J Cereb Blood Flow Metab* 1997;17:1040–1047.
16. Hyder F, Renken R, Rothman DL. In vivo carbon-edited detection with proton echo-planar spectroscopic imaging (ICED PEPSI): $[3,4\text{-}^{13}\text{C}_2]\text{glutamate}/\text{glutamine}$ tomography in rat brain. *Magn Reson Med* 1999;42:997–1003
17. Mason GF, Rothman DL, Behar KL, et al. NMR determination of the TCA cycle rate and alpha-ketoglutarate/glutamate exchange rate in rat brain. *J Cereb Blood Flow Metab* 1992;12:434–447.
18. Mason GF, Gruetter R, Rothman DL, et al. Simultaneous Determination of the rates of the TCA cycle, glucose utilization, alpha-ketoglutarate/glutamate exchange, and glutamine synthesis in human brain by NMR. *J Cereb Blood Flow Metab* 1995;18:12–25.
19. Mason GF, Pan JW, Chu WJ, et al. Measurement of the tricarboxylic acid cycle rate in human gray and white matter in vivo by ^1H - ^{13}C magnetic resonance spectroscopy at 4.1T. *J Cereb Blood Flow Metab* 1999;19:1179–1188.
20. Kunnecke B, Cerdan S, Seelig J. Cerebral metabolism of $[1,2\text{-}^{13}\text{C}]$ glucose and $[\text{U-}^{13}\text{C}]$ 3 hydroxybutyrate in rat brain as detected by ^{13}C NMR spectroscopy. *NMR Biomed* 1993;6:264–277.
21. Van Zijl PMC, Chesnick AS, DesPres D, et al. In vivo proton spectroscopy and spectroscopic imaging of $[1\text{-}^{13}\text{C}]$ glucose and its metabolic products. *Magn Reson Med* 1993;30:544–551.
22. Van Zijl PMC, Chesnick AS, DesPres D, et al. Determination of cerebral glucose transport and metabolic kinetics by dynamic MR spectroscopy. *Am J Physiol* 1997;273:E1216–1217.
23. Lapidot A, Gopher A. Cerebral metabolic compartmentation. Estimation of glucose flux via pyruvate carboxylase/pyruvate dehydrogenase by ^{13}C NMR isotopomer analysis of D- $[\text{U-}^{13}\text{C}]$ glucose metabolites. *J Biol Chem* 1994;269:27198–27208.
24. Manor D, Rothman DL, Mason GF, et al. The rate of turnover of cortical GABA from $[1\text{-}^{13}\text{C}]$ glucose is reduced in rats treated with the GABA-transaminase inhibitor vigabatrin (α -vinyl GABA). *Neurochem Res* 1996;12:1031–1041.
25. Sibson NR, Dhankhar A, Mason GF, et al. In vivo ^{13}C NMR measurement of cerebral glutamine synthesis as evidence for glutamate-glutamine cycling. *Proc Natl Acad Sci USA* 1997;94:2699–2704.
26. Sibson NR, Dhankhar A, Mason GF, et al. Stoichiometric coupling of brain glucose metabolism and glutamatergic neuronal activity. *Proc Natl Acad Sci USA* 1998;95:316–321
27. Sibson NR, Mason GF, Shen J, et al. In vivo ^{13}C NMR measurement of neurotransmitter glutamate cycling, anaplerosis and TCA cycle flux in rat brain during $[2\text{-}^{13}\text{C}]$ glucose infusion. *J Neurochem* 2001;76(4):975–989.
28. Hassel B, Bachelard H, Jones P, et al. Trafficking of amino acids between neurons and glia in vivo, effects of inhibition of glial metabolism by fluoroacetate. *J Cereb Blood Flow Metab* 1997;17:1230–1238.
29. Shen J, Petersen KF, Behar KL, et al. Determination of the rate of the glutamate-glutamine cycle in the human brain by in vivo ^{13}C NMR. *Proc Natl Acad Sci USA* 1999;96:8235–8240.
30. Choi I-Y, Tkac I, Ugurbil K. Noninvasive measurements of $[1\text{-}^{13}\text{C}]$ glycogen content and metabolism in rat brain in vivo. *J Neurochem* 1999;73:1300.
31. Pan JW, Stein DT, Mason GF, et al. Gray and white matter metabolic rate in human brain by spectroscopic imaging. *Magn Reson Med* 2000;44:673–679.
32. Shank RP, Campbell GL. (1984) Alpha-ketoglutarate and malate uptake and metabolism by synaptosomes: further evidence for an astrocyte to neuron metabolic shuttle. *J Neurochem* 1984;42:1153–1161.
33. Schousboe A, Westergaard N, Sonnewald U, et al. Glutamate and glutamine metabolism and compartmentation in astrocytes. *Dev Neurosci* 1993;15:359–366.
34. Peng L, Hertz L. Utilization of glutamine and TCA cycle constituents as precursors for transmitter glutamate and GABA. *Dev Neurosci* 1998;15:367–377.
35. Gruetter R, Seaquist ER, Ugurbil K. In vivo studies of neurotransmitter and amino acid metabolism in human brain. *J Neurochem* 2000;74(suppl):S44.
36. Shen J, Sibson NR, Cline G, et al. ^{15}N NMR spectroscopy studies of ammonia transport and glutamine synthesis in the hyperammonemic rat brain. *Dev Neurosci* 1998;20:438–443.
37. Sibson NR, Shen J, Mason GF, et al. Functional energy metabolism: in vivo ^{13}C NMR evidence for coupling of cerebral glucose consumption and glutamatergic neuronal activity. *Dev Neurosci* 1998;20:321–330.
38. Lebon V, Petersen KF, Cline GW, et al. Measurement of total neuronal/astroglial glutamate-glutamine trafficking and astroglial TCA cycle flux in human cerebral cortex using ^{13}C NMR spectroscopy during the infusion of $[2\text{-}^{13}\text{C}]$ acetate. *J Neurochem* 2001;in press.
39. Patel AB, de Graaf RA, Mason GF, et al. GABAergic and glutamatergic neurotransmitter cycling in the rat cerebral cortex. *Proc Int Soc Magn Reson Med* 2001;in press.
40. Van den Berg CJ, Garfinkel D. A simulation study of brain components. Metabolism of glutamate and related substances in mouse brain. *Biochem J* 1971;123:211–218.
41. Ottersen OP, Zhang N, Walberg F. Metabolic compartmentation of glutamate and glutamine: morphological evidence obtained by quantitative immunocytochemistry in rat cerebellum. *Neuroscience* 1992;46:519–534.
42. Conti F, Minelli A. Glutamate immunoreactivity in rat cerebral cortex is reversibly abolished by 6-diazo-5-oxo-L-norleucine (DON), an inhibitor of phosphate-activated glutaminase. *J Histochem Cytochem* 1994;42:717–726.
43. Chen W, Novotny EJ, Boulware SD, et al. Quantitative measurements of regional TCA cycle flux in visual cortex of human brain using ^1H - $\{^{13}\text{C}\}$ NMR spectroscopy. *Proc Soc Magn Reson* 1994;63.
44. Chen W, Zhu X-H, Gruetter R, et al. Study of oxygen utilization changes in human visual cortex during hemifield stimulation using ^1H - ^{13}C MRS and fMRI. *Proc Int Soc Magn Reson Med* 2000;438.
45. Nowak LG, Sanchez-Vives MV, McCormick DA. Influence of low and high frequency inputs on spike timing in visual cortical neurons. *Cereb Cortex* 1997;7:487–501.
46. Roberts E. Failure of GABAergic inhibition: a key to local and global seizures. *Adv Neurol* 1986;44:319–341.
47. Roberts E. The establishment of GABA as a neurotransmitter. In: Squires RF, ed. *GABA and benzodiazepine receptors*, vol 1. Boca Raton: CRC Press, 1988:1–21.
48. Shank RP, Leo GC, Zielke HR. Cerebral metabolic compartmentation as revealed by nuclear magnetic resonance analysis of D- $[1\text{-}^{13}\text{C}]$ glucose metabolism. *J Neurochem* 1993;61:315–323.
49. Siesjo BK. *Brain energy metabolism*. New York: Wiley, 1978.
50. Rothstein JD, Martin L, Levey AI, et al. Localization of neuronal and glial glutamate transporters. *Neuron* 1994;13:713–725.

51. Tsacopoulos M, Magistretti PJ. Metabolic coupling between glia and neurons. *J Neurosci* 1996;16:877–885.
52. Martinez-Hernandez A, Bell KP, Norenberg MD. Glutamine synthetase: glial localization in brain. *Science* 1977;195:1356–1358.
53. Meister A. Glutamine synthetase from mammalian tissues. *Methods Enzymol* 1985;113:185–199.
54. Wiesinger H. Glia-specific enzyme systems. In: Kettenmann H, Ransom BR, eds. *Neuroglia*. Oxford: Oxford University Press, 1995:488–499.
55. Kvamme E, Torgner IAA, Svenneby G. Glutaminase from mammalian tissues. *Methods Enzymol* 1985;113:241–256.
56. Erecinska M, Silver IA. Metabolism and role of glutamate in mammalian brain. *Prog Neurobiol* 1990;35:245–296.
57. Sonnewald U, Westergaard N, Schousboe A, et al. Direct demonstration by [¹³C]NMR spectroscopy that glutamine from astrocytes is a precursor for GABA synthesis in neurons. *Neurochem Int* 1993;22:19–29.
58. Schousboe A, Westergaard N. Transport of neuroactive amino acids in astrocytes. In: Kettenmann H, Ransom BR, eds. *Neuroglia*. New York: Oxford University Press, 1995:246–258.
59. Maycox PR, Hell JW, Jahn R. Amino acid neurotransmission: spotlight on synaptic vesicles. *Trends Neurosci* 1990;13:83–87.
60. Nicholls DG, Attwell D. The release and uptake of excitatory amino acids. *Trends Pharmacol Sci* 1990;11:462–468.
61. Badar-Goffer RS, Ben-Yoseph O, Bachelard HS, et al. Neuronal-glia metabolism under depolarizing conditions. *Biochem J* 1992;282:225–230.
62. Cooper AJL, Plum F. Biochemistry and physiology of brain ammonia. *Physiol Rev* 1987;67:440–519.
63. Haberg A, Qu Hong, Bakken IJ, et al. In vitro and ex vivo ¹³C-NMR spectroscopy studies of pyruvate recycling in brain. *Dev Neurosci* 1998;20:389–398.
64. Hertz L, Yu AC, Kala G, et al. Neuronal-astrocytic and cytosolic-mitochondrial metabolite trafficking during brain activation, hyperammonemia and energy deprivation. *Neurochem Int* 2000;37:83–102.
65. Reubi JC, Van den Berg C, Cuenod M. Glutamine as a precursor for the GABA and glutamate transmitter pools. *Neurosci Lett* 1978;10:171–174.
66. Rothman DL, Petroff OAC, Behar KL, et al. Localized ¹H NMR measurements of GABA levels in human brain in vivo. *Proc Natl Acad Sci USA* 1993;90:5662–5666.
67. Dejong CHC, Kampman MT, Deutz NEP, et al. Cerebral cortex ammonia and glutamine metabolism during liver insufficiency-induced hyperammonemia in the rat. *J Neurochem* 1992;59:1071–1079.
68. Berl S, Takagaki G, Clarke DD, et al. Carbon dioxide fixation in the brain. *J Biol Chem* 1962;237:2570–2573.
69. Kanamori K, Ross BD. ¹⁵N n.m.r. measurement of the in vivo rate of glutamine synthesis and utilization at steady state in the brain of the hyperammonemic rat. *Biochem J* 1993;293:461–468.
70. Kanamori K, Ross BD. In vivo activity of glutaminase in the brain of hyperammonemic rats measured in vivo by ¹⁵N nuclear magnetic resonance. *Biochem J* 1995;305:329–336.
71. Hawkins RA, Miller AL, Nielsen RC, et al. The acute action of ammonia on rat brain metabolism in vivo. *Biochem J* 1973;134:1001–1008.
72. Cheng S. CO₂ fixation in the nervous tissue. *Int Rev Neurobiol* 1971;14:125–157.
73. Fitzpatrick SM, Hetherington HP, Behar KL, et al. Effects of acute hyperammonemia on cerebral amino acid metabolism and pH_i in vivo, measured by ¹H and ³¹P NMR. *J Neurochem* 1989;2:741–479.
74. Kanamatsu T, Tsukada Y. Effects of ammonia on the anaplerotic pathway and amino acid metabolism in the brain: an ex vivo ¹³C NMR spectroscopic study of rats after administering [2-¹³C]glucose with or without ammonium acetate. *Brain Res* 2000;841:11–19.
75. Jones JG, Naidoo R, Sherry AD, et al. Measurement of gluconeogenesis and pyruvate recycling in the rat liver: a simple analysis of glucose and glutamate isotopomers during metabolism of [1,2,3-(¹³C)]propionate. *FEBS Lett* 1997;412:131–137.
76. Schousboe A, Westergaard N, Sonnewald U, et al. Regulatory role of astrocytes for neuronal biosynthesis and homeostasis of glutamate and GABA. *Prog Brain Res* 1992;94:199–211.
77. Yudkoff M, Nissim I, Daikhin Y, Lin ZP, et al. Brain glutamate metabolism: neuronal-astroglial relationships. *Dev Neurosci* 1993;15:343–350.
78. Danbolt NC, Storm-Mathisen J, Kanner BI. An [Na⁺-K⁺] coupled L-glutamate transporter purified from rat brain is located in glial cell processes. *Neuroscience* 1992;51:295–310.
79. Kanner BI, Sharon I. Active transport of L-glutamate by membrane vesicles isolated from rat brain. *Biochemistry* 1978;17:3949–3953.
80. Pines G, Kanner BI. Counterflow of L-glutamate in plasma membrane vesicles and reconstituted preparations from rat brain. *Biochemistry* 1990;29:11209–11214.
81. Chaudhry FA, Lehre KP, van Lookeren Campagne M, et al. Glutamate transporters in glial plasma membranes: highly differentiated localizations revealed by quantitative ultrastructural immunocytochemistry. *Neuron* 1995;15:711–720.
82. Lehre KP, Levy LM, Ottersen OP, et al. Differential expression of two glial glutamate transporters in the rat brain: quantitative and immunocytochemical observations. *J Neurosci* 1995;15:1835–1853.
83. Milton ID, Banner SJ, Ince PG, et al. Expression of the glial glutamate transporter EAAT2 in the human CNS: an immunohistochemical study. *Mol Brain Res* 1997;52:17–31.
84. Rothstein JD, Jin L, Dykes-Hoberg M, et al. Chronic inhibition of glutamate uptake produces a model of slow neurotoxicity. *Proc Natl Acad Sci USA* 1993;90:6591–6595.
85. Rothstein JD, Dykes-Hoberg M, Pardo CA, et al. Knockout of glutamate transporters reveal a major role for astroglial transport in excitotoxicity and clearance of glutamate. *Neuron* 1996;16:675–686.
86. Ginsberg SD, Martin LJ, Rothstein JD. Regional deafferentation down-regulates subtypes of glutamate transporter proteins. *J Neurochem* 1995;65:2800–2803.
87. Ginsberg SD, Rothstein JD, Price DL, et al. Fimbria-fornix transections selectively down-regulate subtypes of glutamate transporter and glutamate receptor proteins in septum and hippocampus. *J Neurochem* 1996;67:1208–1216.
88. Bergles DE, Jahr CE. Synaptic activation of glutamate transporters in hippocampal astrocytes. *Neuron* 1997;9:1297–1308.
89. Pellerin L, Pellegrini G, Bittar PG, et al. Evidence supporting the existence of an activity dependent astrocyte neuron lactate shuttle. *Dev Neurosci* 1998;20:291–299.
90. Magistretti PJ, Pellerin L, Rothman DL, et al. Energy on demand. *Science* 1999;283:496–497.
91. Pellerin L, Magistretti PJ. Glutamate uptake into astrocytes stimulates aerobic glycolysis: a mechanism coupling neuronal activity to glucose utilization. *Proc Natl Acad Sci USA* 1994;91:10625–10629.
92. Hertz L, Swanson RA, Newman GC, et al. Can experimental conditions explain the discrepancy over glutamate stimulation of aerobic glycolysis? *Dev Neurosci* 1998;20:339–347.
93. Fell DA. Metabolic control analysis: a survey of its theoretical and experimental development. *Biochem J* 1997;286:313–330.
94. Martin DL. The role of glia in the inactivation of neurotransmit-

- ters. In: Kettenmann H, Ransom BR, eds. *Neuroglia*. Oxford: Oxford University Press, 1995:732–745.
95. Kadekaro M, Crane AM, Sokoloff L. Differential effects of electrical stimulation of sciatic nerve on metabolic activity in spinal cord and dorsal root ganglion in the rat. *Proc Natl Acad Sci USA* 1985;82:6010–6013.
 96. Kennedy C, Des Rosiers MH, Sakurada O. Metabolic mapping of the primary visual system of the monkey by means of the autoradiographic [¹⁴C] deoxyglucose technique. *Proc Natl Acad Sci USA* 1976;73:4230–4234.
 97. Yarowsky P, Kadekaro M, Sokoloff L. Frequency-dependent activation of glucose utilization in the superior cervical ganglion by electrical stimulation of cervical sympathetic trunk. *Proc Natl Acad Sci USA* 1983;80:4179–4183.
 98. Bachelard H. Landmarks in the application of ¹³C-Magnetic Resonance Spectroscopy to studies of neuronal/glia relationships. *Dev Neurosci* 1998;20:277–188.
 99. Ruderman NB, Ross PS, Berger M, et al. Regulation of glucose and ketone-body metabolism in brain of anaesthetized rats. *Biochem J* 1974;138:1–10.
 100. Pan JW, Rothman DL, Behar KL, et al. Human brain beta-hydroxybutyrate and lactate increase in fasting induced ketosis. *J Cereb Blood Flow* 2000; *in press*.
 101. Meldrum BS. GABAergic mechanism in the pathogenesis and treatment of epilepsy. *Br J Clin Pharmacol* 1989;27:3S–11S.
 102. Olsen RW, Avoli M. GABA and epileptogenesis. *Epilepsia* 1997;38:399–407.
 103. Behar KL, Rothman DL, Spencer DD, et al. Analysis of macromolecule resonances in ¹H NMR spectra of human brain. *Magn Reson Med* 1994;32:294–302.
 104. Hetherington HP, Newcomer BR, Pan JW. Measurement of human cerebral GABA at 4.1 T using numerically optimized editing pulses. *Magn Reson Med* 1998;39:6–10.
 105. Shen J, Shungu DC, Rothman DL. In vivo chemical shift imaging of γ -aminobutyric acid in the human brain. *Magn Reson Med* 1999;41:35–42.
 106. Behar KL, Boehm D. Measurement of GABA following GABA-transaminase inhibition by gabaculine: a ¹H and ³¹P NMR spectroscopic study of rat brain in vivo. *J Cereb Blood Flow Metab* 1991;11(suppl 2):S783.
 107. Preece NE, Williams SR, Jackson G, et al. ¹H-NMR studies of vigabatrin-induced increases in cerebral GABA. *Proc Soc Mag Reson Med* 1991;1000.
 108. Petroff OAC, Rothman DL, Behar KL, et al. Human brain gamma-aminobutyric acid (GABA) levels and seizure control following initiation of vigabatrin therapy. *J Neurochem* 1996;67:2399–2404.
 109. Petroff OAC, Behar KL, Rothman DL. New NMR measurements in epilepsy. Measuring brain GABA in patients with complex partial seizures. *Adv Neurol* 1999;79:945–951.
 110. Petroff OAC, Rothman DL. Measuring human brain GABA in vivo: effects of GABA-transaminase inhibition with vigabatrin. *Mol Neurobiol* 1998;16:97–121.
 111. Petroff OAC, Hyder F, Rothman DL, et al. Functional imaging in the epilepsies proton MRS: GABA and glutamate. *Adv Neurol* 2000;83:263–272.
 112. Rothman DL, Behar KL, Prichard JW, et al. Homocarnosine and the measurement of neuronal pH in patients with epilepsy. *Magn Reson Med* 1997;32:924–929.
 113. Martin DL, Rimvall K. Regulation of γ -aminobutyric acid synthesis in the brain. *J Neurochem* 1993;60:395–407.
 114. Martin DL, Liu H, Martin SB, et al. Structural features and regulatory properties of the brain glutamate decarboxylases. *Neurochem Int* 2000;37:111–119.
 115. Kaufman DL, Houser CR, Tobin AJ. Two forms of the gamma-aminobutyric acid synthetic enzyme glutamate decarboxylase have distinct intraneuronal distributions and cofactor interactions. *J Neurochem* 1991;56:720–723.
 116. Rimvall K, Martin DL. The level of GAD₆₇ protein is highly sensitive to small increases in intraneuronal gamma-aminobutyric acid levels. *J Neurochem* 1994;62:1375–1381.
 117. Sheikh SN, Martin DL. Elevation of brain GABA levels with vigabatrin (gamma-vinylGABA) differentially affects GAD₆₅ and GAD₆₇ expression in various regions of rat brain. *J Neurosci Res* 1998;52:736–741.
 118. Asada H, Kawamura Y, Maruyama K, et al. Mice lacking the 65 kDa isoform of glutamic acid decarboxylase (GAD₆₅) maintain normal levels of GAD₆₇ and GABA in their brains but are susceptible to seizures. *Biochem Biophys Res Commun* 1996;229:891–895.
 119. Asada H, Kawamura Y, Maruyama K, et al. Cleft palate and decreased brain γ -aminobutyric acid in mice lacking the 67-kDa isoform of glutamic acid decarboxylase. *Proc Natl Acad Sci USA* 1996;94:6496–6499.
 120. Petroff OAC, Rothman DL, Behar KL, et al. Low brain GABA level is associated with poor seizure control. *Ann Neurol* 1996;40:908–911.
 121. Petroff OAC, Hyder F, Mattson RH, et al. Topiramate increases brain GABA, homocarnosine, and pyrrolidinone in patients with epilepsy. *Neurology* 1999;52:473–478.
 122. Petroff OAC, Hyder F, Rothman DL, et al. Effects of gabapentin on brain GABA, homocarnosine, and pyrrolidinone in epilepsy. *Epilepsia* 2000;41:675–680.
 123. Hetherington HP, Kuzniecky RI, Pan JW. Acute and chronic alterations in human cerebral GABA levels in response to topiramate, lamotrigine, and gabapentin. *Proc Soc Magn Reson Med* 1998;1:542.
 124. Kuzniecky RI, Hetherington HP, Ho S, et al. Topiramate increases cerebral GABA in healthy humans. *Neurology* 1998;51:627–629.
 125. Petroff OAC, Rothman DL, Behar KL, et al. The effect of gabapentin on brain gamma-aminobutyric acid in patients with epilepsy. *Ann Neurol* 1996;39:95–99.
 126. Novotny EJ, Hyder F, Rothman DL. GABA changes with vigabatrin in the developing human brain. *Epilepsia* 1998;40:462–466.
 127. Kocsis JD, Mattson RH. GABA levels in the brain: a target for new antiepileptic drugs. *Neuroscientist* 1996;6:326–334.
 128. Richerson GB, Gasparly HL. Carrier-mediated GABA release: Is there a functional role? *Neuroscientist* 1987;3:151–157.
 129. Sanacora G, Mason GF, Rothman DL, et al. Preliminary evidence of reduced cortical GABA levels in depressed patients assessed using ¹H-magnetic resonance spectroscopy. *Arch Gen Psychiatry* 1999;56:1043.
 130. Behar KL, Rothman DL, Petersen KF, et al. Preliminary evidence of reduced cortical GABA levels in localized 1-H-MR spectra of alcohol-dependent and hepatic encephalopathy patients. *Am J Psychiatry* 1999;156:952–954.
 131. Hyder F, Petroff OAC, Mattson RH, et al. Localized ¹H NMR measurements of 2-pyrrolidinone in human brain in vivo. *Magn Reson Med* 1999;41:889–896.
 132. Fox PT, Raichle ME, Mintun MA, et al. Nonoxidative glucose consumption during focal physiologic neural activity. *Science* 1988;241:462–464.
 133. Gjedde A. The energy cost of neuronal depolarization. In: Gulyas B, Ottoson D, Roland PE, eds. *Functional organisation of the human visual cortex*. Wenner-Gren International Symposium Series, vol 61. Oxford: Pergamon Press, 1993:291–306.
 134. Ogawa S, Menon RS, Kim SG, et al. On the characteristics of functional magnetic resonance imaging of the brain. *Annu Rev Biophys Biomol Struct* 1998;27:447–474.

135. Hyder F, Shulman RG, Rothman DL. Regulation of cerebral oxygen delivery. *Adv Exp Med Biol* 1999;471:99–109
136. Prichard JW, Rothman DL, Novotny EJ, et al. Lactate rise detected by ¹H NMR in human visual cortex during physiological stimulation. *Proc Natl Acad Sci USA* 1991;88:5829–5831
137. Sappey-Mariniere D, Calabrese G, Fein G, et al. Effect of photic stimulation on human visual cortex lactate and phosphates using ¹H and ³¹P magnetic resonance spectroscopy. *J Cereb Blood Flow Metab* 1992;12:584–592.
138. Frahm J, Kruger G, Merboldt KD, et al. Dynamic uncoupling and recoupling of perfusion and oxidative metabolism during focal brain activation in man. *Magn Reson Med* 1996;35:143–148.
139. Shulman RG. Functional imaging studies: linking mind and basic neuroscience. *Am J Psychiatry* 2001;158:11–20.
140. Ueki M, Linn F, Hossman KA. Functional activation of cerebral blood flow and Metabolism before and after global ischemia of rat brain. *J Cereb Blood Flow Metab* 1988;8:486–494.
141. Hyder F, Kennan RP, Kida I, et al. Dependence of oxygen delivery on blood flow in rat brain: a 7 Tesla nuclear magnetic resonance study. *J Cereb Blood Flow Metab* 2000;20:485–498.
142. Marrett S, Gjedde A. Changes of blood flow and oxygen consumption in visual cortex of living humans. *Adv Exp Med Biol* 1997;413:205–208.
143. Davis TL, Kwong KK, Weisskoff RM, et al. Calibrated functional MRI: mapping the dynamics of oxidative metabolism. *Proc Natl Acad Sci USA* 1998;95:1834–1839.
144. Reivich M, Alavi A, Gur RC. Positron emission tomographic studies of perceptual tasks. *Ann Neurol* 1984;15:S61–S65.
145. Hoge RD, Atkinson J, Gill B, et al. Linear coupling between cerebral blood flow and oxygen consumption in activated human cortex. *Proc Natl Acad Sci USA* 1999;96:9403–9408.
146. Kim SG, Rostrup E, Larsson HB, et al. Determination of relative CMRO₂ from CBF and BOLD changes: significant increase of oxygen consumption rate during visual stimulation. *Magn Reson Med* 1999;41:1152–1161.
147. Kim SG, Ugurbil K. Comparison of blood oxygenation and cerebral blood flow effects in fmri: estimation of relative oxygen consumption change. *Magn Reson Med* 1997;38:59–65.
148. Borgstrom L, Chapman AG, Siesjo BK. Glucose consumption in the cerebral cortex of rat during bicuculline-induced status epilepticus. *J Neurochem* 1976;27:971–973.
149. Marret S, Fujita H, Meyer E, et al. Stimulus specific increase of oxidative metabolism in human visual cortex. In: Uemura K, Lassen NA, Jones T, eds. *Quantification of brain function: tracer kinetics and image analysis in brain PET*. Amsterdam: Elsevier, 1993:217–224.
150. Sibson NR, Rothman DL, Behar KL, et al. The glycogen shunt and brain energetics. *Proc Int Soc Magn Reson Med* 1999;1:730.
151. Shulman RG, Rothman DL. The “glycogen shunt” in exercising muscle: a novel role for glycogen in muscle energetics and fatigue. *Proc Natl Acad Sci USA* 2001;98:457–461.
152. Dienel GA, Wang RY, Cruz NF. Channeling of ¹⁴C glucose into tricarboxylic acid cycle derived metabolic pools in neurons and glia during and after sensory stimulation. Proceedings of the International Society for Neurochemistry 3rd International Conference on Brain Energy Metabolism, 1997.
153. Swanson RA, Morton MM, Sagar SM, et al. Sensory stimulation induces local cerebral glycogenolysis: demonstration by autoradiography. *Neuroscience* 1992;51:451–461.
154. Magistretti PJ, Sorg O, Martin J-L. Regulation of glycogen metabolism in astrocytes: physiological, pharmacological and pathological aspects. In: Murphy S, ed. *Astrocytes: pharmacology and function*. San Diego: Academic Press, 1993:243–265.
155. Price TB, Taylor R, Mason GM, et al. Turnover of human muscle glycogen during low-intensity exercise. *Med Sci Sports Exerc* 1994;26(8):983–991.
156. Hyder F, Shulman RG, Rothman DL. A model for the regulation of cerebral oxygen delivery. *J Appl Physiol* 1998;85:554–564.
157. Shulman RG, Rothman DL, Hyder F. Stimulated changes in localized cerebral energy consumption under anesthesia. *Proc Natl Acad Sci USA* 1999;96:3245–3250.
158. Hyder F, Shulman RG, Rothman DL, et al. Localized energetic changes with brain activation from anesthesia II: relative BOLD changes at 7T. *Proc Int Soc Magn Reson Med* 2000;8:968.
159. Posner MI, Raichle ME. *Images of mind*. New York: Freeman, 1994.
160. Buchsbaum M, Hazlett EA. Positron emission tomography studies of abnormal glucose metabolism in schizophrenia. *Schizophr Bull* 1998;24(3):343–364.
161. Smith EE. Infusing cognitive neuroscience into cognitive psychology. In: Solso RL, ed. *Mind and brain sciences in the 21st century*. A Bradford Book, MIT Press, 1997:71–89.
162. Frackowiack RSJ, Friston KJ, Frith CD, et al. *Human brain function*. San Diego: Academic Press, 1997:25–41.
163. Jennings JM, McIntosh AR, Kapur S, et al. Cognitive subtractions may not add up: the interaction between semantic processing and response mode. *Neuroimage* 1997;5:229–239.
164. Luck SJ, Cheazzi L, Hillyard SA, et al. Neural mechanisms of spatial selective attention in areas V1, V2, and V4 of macaque visual cortex. *J Neurophysiol* 1997;77(1):24–42.
165. Kastner S, DeWeerd P, Desimone R, et al. Mechanisms of directed attention in the human extrastriate cortex as revealed by functional MRI. *Science* 1998;282:108–111.
166. Chawla D, Rees G, Friston KJ. The physiological basis of attentional modulation in extrastriate visual areas. *Nature Neurosci* 1999;2:671–676.
167. Tsodyks M, Kenet T, Grinvald A, et al. Linking spontaneous activity of single cortical neurons and the underlying functional architecture. *Science* 1999;286:1943–1946.
168. Singer W. Putative functions of temporal correlations in neocortical processing. In: Koch C, David JL, eds. *Large scale neuronal theories of the brain*. MIT Press, 1994:201–238.